Sensors **2015**, *15*, 17115-17148; doi:10.3390/s150717115

OPEN ACCESS
sensors
ISSN 1424-8220
www.mdpi.com/journal/sensors

Review

Optical Fibre Pressure Sensors in Medical Applications

Sven Poeggel [1,*], Daniele Tosi [2], DineshBabu Duraibabu [1], Gabriel Leen [1], Deirdre McGrath [3] and Elfed Lewis [1,*]

[1] Optical Fibre Sensors Research Centre, University of Limerick, Limerick, Ireland;
E-Mails: ddineshbabu@hotmail.com (D.D.); Gabriel.leen@ul.ie (G.L.)
[2] School of Engineering, Nazarbayev University, Astana 010000, Kazakhstan;
E-Mail: daniele.tosi@nu.edu.kz
[3] Graduate Entry Medical School, University of Limerick, Limerick, Ireland;
E-Mail: Deirdre.McGrath@ul.ie

* Authors to whom correspondence should be addressed; E-Mails: Sven@Poeggel.eu (S.P.);
Elfed.Lewis@ul.ie (E.L.); Tel./Fax: +353-89-4580-007(S.P.).

Academic Editor: Lorenzo Pavesi

Received: 1 June 2015 / Accepted: 2 July 2015 / Published: 15 July 2015

Abstract: This article is focused on reviewing the current state-of-the-art of optical fibre pressure sensors for medical applications. Optical fibres have inherent advantages due to their small size, immunity to electromagnetic interferences and their suitability for remote monitoring and multiplexing. The small dimensions of optical fibre-based pressure sensors, together with being lightweight and flexible, mean that they are minimally invasive for many medical applications and, thus, particularly suited to *in vivo* measurement. This means that the sensor can be placed directly inside a patient, e.g., for urodynamic and cardiovascular assessment. This paper presents an overview of the recent developments in optical fibre-based pressure measurements with particular reference to these application areas.

Keywords: optical fibre sensors; Fabry–Perot interferometer; pressure sensors

---

1. Introduction

The pressure in a living human body is influenced by internal (e.g., muscles, fluids) and external (e.g., gravity, atmospheric) forces. The measurement of pressure and forces *in vivo* is a key asset in a

range of biomedical applications, including cardiovascular and urologic diagnostic procedures, surgical procedures and monitoring of invasive treatments [1].

The most popular devices currently used for medical pressure measurement are based on catheters and guidewires. Air-charged catheters are low-cost and popular, particularly for urology applications [2]. Fluid-filled catheters represent a valuable alternative with a more stable response and are very popular in urology [3,4] and cardiovascular [5,6] applications. The work of Cooper *et al.* [3] compared the pressure response of air-charged and fluid-filled catheters. They demonstrated that air-charged catheters act as an overdamped system, whereas water-filled catheters act as an underdamped system. Pressure guidewires represent a modern alternative to catheters, having a smaller footprint and higher cost [7,8]. Guidewires and catheter pressure transducers are based on the principle of electro-mechanical pressure transducers [9–11]. Often, the pressure-sensing device is integrated in a complex catheterization, with multiple functionalities [12]. Commercial products are well established in urology and cardiovascular applications.

An alternative to these electro-mechanical pressure sensors, the optical fibre pressure sensor (OFPS) has become increasingly common in the medical field. This overview is intended for: (1) medical doctors to introduce them to the topic of OFPS; and (2) for engineers with a view toward understanding the demand for pressure sensor technology within the medical environment and the medical applications of current available technologies. The aim of this review therefore is to describe the use of the optical fibre pressure sensors applied in medicine with particular focus on the current state-of-the-art in technology and developments in the context of several applications, including those that are currently established and emerging in the medical field.

The paper is arranged as followed: Section 2 describes pressure measurement requirements within the relevant medical areas of interest (e.g., cardiology, urology, *etc.*) and the working principles of existing pressure sensors. Section 3 gives an introduction to optical fibre pressure sensors and provides details of the technology involved. Section 4 provides an overview of OFPS in biomedical applications and commercial products. Section 5 comprises a conclusion on the technologies reported.

2. Pressure Sensors in Medicine

In the medical field, a sensor represents a device that responds to a physical stimulus and transmits a resulting impulse. Therefore, the fundamental purpose of a sensor system is to accurately measure a signal that enables the well being of a patient to be determined. The human and animal organism is a complex combination of a variety of organs, bones, joints and muscles (Figure 1 [13,14]). Each body part has its own set of characteristics (e.g., volume, structure, inner pressure, *etc.*). Additionally, each component may undergo a unique dynamic change in pressure, either due to normal physiological changes or as a result of an underlying pathophysiological process during the course of an illness. Clausen and Glott [15] recommended dividing the body pressures into three domains: (1) low pressure regions (e.g., capillaries and brain); (2) medium pressure regions (e.g., heart and lung); and (3) high pressure regions/states (e.g., joints and pressure changes during ablation techniques).

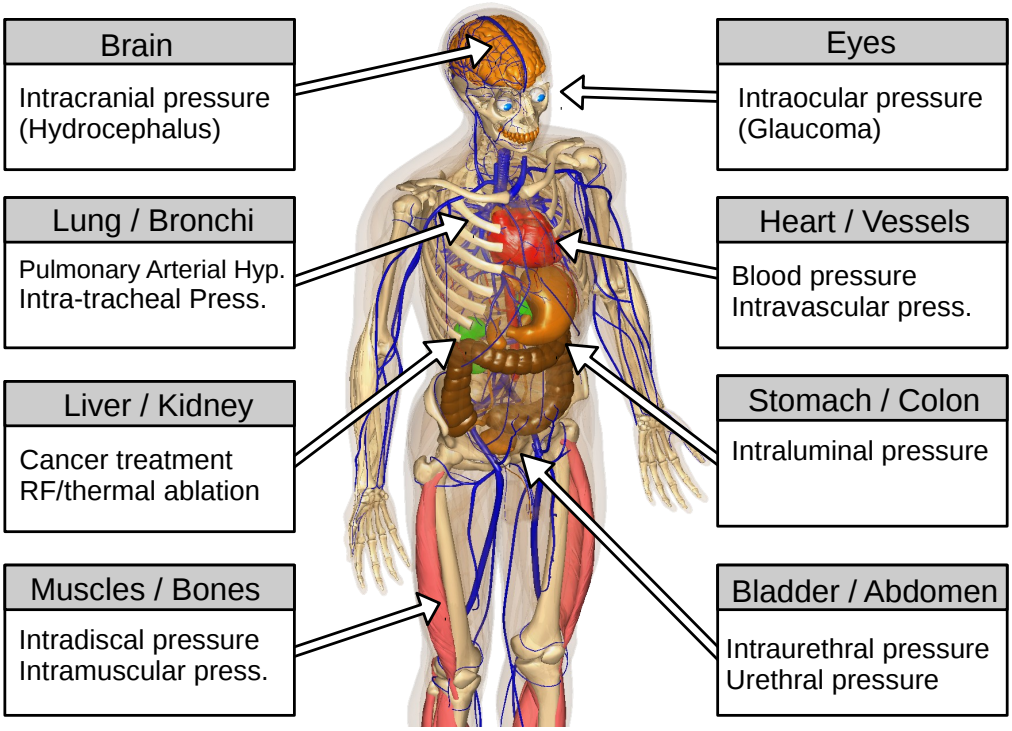

Figure 1. Body parts with pressure measurements and the relevant underlying physiological/pathophysiological condition associated with each organ/tissue (created in bodyparts3d [13,14]).

The requirements for a particular pressure sensor technology depend strongly on the area of interest (urology, cardiovascular, *etc.*), the place of measurement (e.g., organ, bone or muscle) or the method for which the sensor is employed (single point measurement, cancer treatment or long-term observation). Furthermore, any sensor or sensor system adopted for physiological measurement in the human body must meet certain fundamental standards of the suitability of use. Such standards are generally defined by an authorization institute, such as the Food and Drug Administration (FDA) and by the International Organization for Standardization (ISO), with particular reference to ISO 10993 [16] (Biological Evaluation of Medical Devices Part 1: Evaluation and Testing) and ISO 13485 [17] (Medical devices—Quality management systems—Requirements for regulatory purposes).

2.1. Technical Pressure Sensor Requirements

There are technical standards that must be met for each specific task, e.g., in the case of cardiology pressure analysis, standards defined by Association for the Advancement of Medical Instrumentation (AAMI) (in ISO 81060-2) [18], must be met when using sensors and devices in this setting. These standards are also FDA approved [19].

Range is the difference between the minimal to maximal pressure values measured in the body cavity. The pressure range can vary in normal physiological states from a large range 0–20 kPa (0–150 mmHg) in the case of left ventricular pressure to narrow ranges 0–1 kPa (0–7.5 mmHg) in the case of intra-cranial pressure. In diseased or pathophysiological states, pressure can fall as low as –10 kPa (–75 mmHg) in the case of intra-alveolar and intra-tracheal pressure and can rise as high as 40 kPa (300 mmHg) for

aortic and left ventricular pressure. The diastolic pressure in a relaxed blood vessel has a normal range of 60–80 mmHg and can be elevated as high as 90–120 mmHg in a systolic contracted blood vessel [1].

The AAMI demands a pressure range of –4 kPa (–30 mmHg) to 40 kPa (300 mmHg) for a blood pressure transducer. Additionally, it should not be damaged with an overpressure in the range of –53 kPa (–400 mmHg) to 533 kPa (4000 mmHg) [20,21].

Accuracy (includes resolution), in terms of sensor requirements, often depends on the area of interest (e.g., heart, bone or muscle). A typical example arises in the case of blood pressure measurement, where for every 2.6-kPa (20 mmHg) increase in systolic pressure or 1.3 kPa (10 mmHg) in diastolic pressure, the mortality from ischemic heart disease and stroke doubles [22,23]. A small variation in blood pressure therefore can distinguish between a well, normotensive patient and a patient who is ill. For example, an adult can suffer from chronic disease (Table 1 [22]), where each stage is defined by a threshold of 133 Pa (1 mmHg). A high blood pressure value can be measured in proximal aorta. However, this blood pressure decreases as one moves away from the aorta to the femoral artery, radial artery and, subsequently, to the arterioles, becoming very small in the capillaries [24].

Table 1. Classification and management of blood pressure [22].

Blood Pressure (BP) Classification	Diastolic	Systolic	Treatment
Normal:	<80 mmHg	<120 mmHg	Normal
Prehypertension:	80–89 mmHg	120–139 mmHg	No antihypertensive drug
Hypertension Stage 1	90–99 mmHg	140–159 mmHg	ACE, ARB, β-blocker
Hypertension Stage 2	>100 mmHg	>160 mmHg	2-Drug combination

The American National Standards Institute (ANSI)/AAMI BP22:1994 (2006) therefore dictates that the accuracy for blood pressure measurement should be better than ±1% in the range of –4 kPa (–30 mmHg) to 6.7 kPa (50 mmHg) and ±3% in the range of 6.7 kPa (50 mmHg) to 40 kPa (300 mmHg) [21,23].

The sampling rate is the number of measurements acquired in one second and depends on the periodicity and waveform of the pressure signal. The fundamental natural frequency (f_n) in a heartbeat rate up to 120 $\frac{\text{beats}}{\text{s}}$ is $f_n = 0.5$ Hz. However, the complex waveform requires further harmonics to rebuild the correct shape. With respect to Nyquist's theorem [25], a system should acquire at least double the highest frequency present in the signal, to preserve the signal. In practice, a medical sensor should acquire 5–10-times more samples than the highest frequency [26]. Further investigation allows an additional filtering and/or down sampling to analyse the important frequency band.

Since most internally-deployed sensors in medicine are placed in a catheter, with the function of either housing the sensor or working as a transducer, this may affect the frequency response. Gardner [27] demonstrated the affect of a catheter on the shape of a heart pulse in which the catheter is treated as a second-order system (with elasticity, mass and friction) having a natural frequency and damping factor. Gardner demonstrated that an overdamped catheter would not detect the dicrotic notch of a single heart beat, and an underdamped catheter would result in a noisily (incorrectly)-formed shape, thereby altering the accuracy of the pressure measurement. The AAMI therefore recommended a minimum frequency (200 Hz) for devices monitoring blood pressure [21].

Table 2. Collection of exemplary standards for medical pressure analysis. ICP, intra-cranial pressure; AAMI, Association for the Advancement of Medical Instrumentation; ERS, European Respiratory Society; ATS, American Thoracic Society.

Area (Technique)	Body Part	Min. Pressure	Max. Pressure	Pressure Resolution	Sampling (Frequency)	Additional	Reference
Cardiology (BP Monitoring)	Heart, Veins, Arteries	–4 kPa (–30 mmHg)	40 kPa (300 mmHg)	13 Pa (0.1 mmHg)	200 Hz	Volume restricted	AAMI BP22 [21]
Urology (Cystometry)	Bladder, Abdomen	0 Pa (0 cmH_2O)	25 kPa (250 cmH_2O)	50 Pa (0.5 cmH_2O)	10 Hz	Differential measurement	Schaefer *1 [28] and [29–31]
Neurology (ICP Monitoring)	Brain, Skull, Dural Tissue	0 Pa (0 mmHg)	13.3 kPa (100 mmHg)	260 Pa (2 mmHg)	-	Sterilization	AAMI NS28 [32], Andrew *et al.* [33]
Pulmonology (Transpulmonary)	Respiratory Tract, Lungs	–10 kPa (–100 cmH_2O)	15 kPa (150 cmH_2O)	2–40 Pa (4 mmH_2O)	200 Hz (10 Hz)	Temperature, humidity	ERS/ATS [34,35] Bensenor [36]
Gastroenterology (Manometry)	Stomach, Colon	0 Pa (0 mmHg)	13.3 kPa (100 mmHg)	-	8 Hz	Multi probes (6 or more)	RAO *et al.* [37] Cross-Adame [38]
Ophthalmology (Tonometry)	Eyes	0 Pa (0 cmH_2O)	8 kPa (60 mmHg)	13 Pa (0.1 mmHg)	100 Hz	Volume restricted	Weinreb [39] ISO 8612 [40]
Rheumatology	Muscle, Bones, Spine	0 kN *2	3 kN *2	-	-	High pressure	ISO 14242-2 [41]
Cancer Treatment (Ablation)	Full Body	0 kPa *3	200 kPa *3	-	-	Temperature, RF-field	

*1 The recommendation by Schaefer *et al.* was also used by the NHS Purchasing and Supply Agency (U.K.), for their official buyers guide for urodynamic systems (CEP08045) [42]. *2 Instead of pressure, the weight distribution is of interest. It is mentioned here, as well, since the same principles can be used. *3 The lack of research in this field has complicated a determined standardization. The values are based on observation by preliminary tests.

Additional pressure sensor requirements are dependent on the specific task. For example, in small vessels, an *in vivo* pressure sensor with a large diameter can effect the measurement by restricting the blood flow. Furthermore, the magnetic field in a magnetic resonance imaging (MRI) can impair electrical sensors. In radio-frequency (RF) ablation techniques, the high intensity of electromagnetic radiation-generated temperature can impair and, in some cases, destroy the pressure sensor. Innovative adaptive techniques therefore are necessary in such circumstances. A list of requirements for specific medical fields are therefore shown in Table 2.

2.2. Principles of Pressure Sensors

The two principles of pressure measurement are exemplified by the classical strain gauge transducer and diaphragm displacement sensor [43], equally applicable in the case of optical fibre sensors (OFS). These principles will be explained in the following.

Strain gauge transducers are characterised as those that exhibit a change in their output parameter in response to the measurand (*i.e.*, strain), e.g., electrical resistance (Figure 2a) or wavelength in optical sensors. The gauge factor (*i.e.*, sensitivity), in Equation (1), is determined by the relative change of resistance ($\Delta R/R$) with respect to the relative change of the length ($\Delta L/L$) (also called strain ϵ). In an electrical sensor, the change in resistance can be most effectively measured using a Wheatstone bridge [44,45].

$$\mathrm{GF} = \frac{\Delta R/R}{\Delta L/L} = \frac{\Delta R/R}{\epsilon} \tag{1}$$

Diaphragm displacement sensors are based on micro-electromechanical systems (MEMS) technology, in which sensors have a bendable flat surface (*i.e.*, the diaphragm) on a sealed cavity. The diaphragm bends (deforms) according to the change of pressure and can be capacitance based or based on a piezoelectric transducer. The sensor structure is shown schematically in Figure 2b. In the initial state, the cavity has an initial volume (V_0) and pressure (P_0). Since the cavity is sealed, a change in pressure (ΔP) causes the medium (e.g., air) inside the cavity to compress/expand (ΔV).

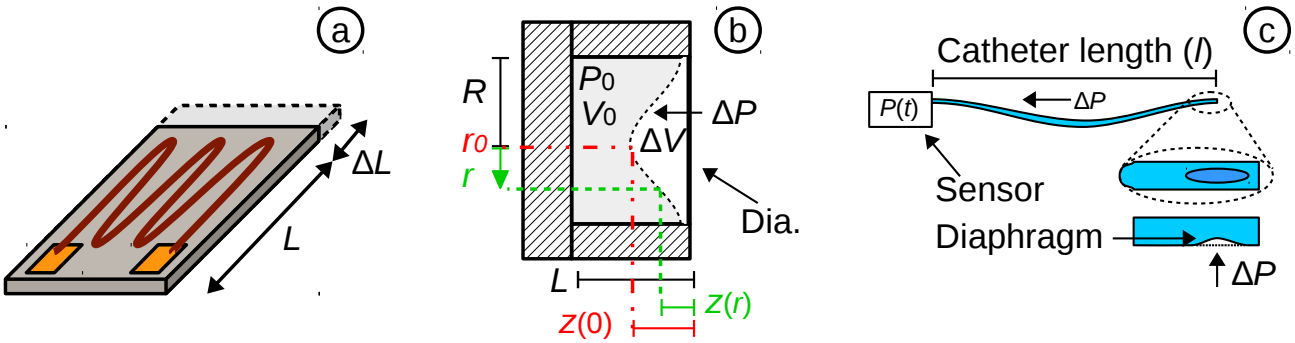

Figure 2. (**a**) Schematic of a piezoresistive sensor; (**b**) schematic of a diaphragm displacement sensor; (**c**) water-filled catheter as the pressure transducer.

In the case of a circular cross-section diaphragm with clamped edges, the bending of the diaphragm ($z(r)$) can be theoretically predicted using Equation (2), provided the bending displacement is limited to less than 30% of the diaphragm thickness (h). This principle is used for capacitive and piezoresistive sensors. In the centre of the diaphragm ($r = 0 = r_0$), the bending displacement is at maximum. Whereas on the clamped edge ($r = R$), no bending occurs ($z(R) = 0$). The elasticity depends on Poisson's ratio (μ) and Young's modulus (E) of the diaphragm material. The displacement of the diaphragm can be measured by a frequency-excited gain circuit [1].

$$z(r) = \frac{3}{16} \cdot \frac{(1-\mu^2)(R^2-r^2)}{Eh^3} \cdot \Delta P \tag{2}$$

Catheter-based pressure systems use a catheter filled with an incompressible medium (e.g., water or saline solution), connected to a pressure sensor (Figure 2c). A change in pressure at the tip of the catheter results in a deformation of the diaphragm, which compresses or decompresses the water and, hence, transmits the pressure directly to the connected sensor. The natural frequency (f_0) of a water-filled catheter (with a density of ρ) can be calculated by Equation (3). Togawa *et al.* [1] demonstrated the limitation of the water-filled transducer. For standard-sized medical catheters [46,47], with an outer diameter (o.d.) $r_0 = 1.66$ mm (5 Fr), an inner diameter (i.d.) of $r_i = 0.66$ mm (2 Fr) and a length of $l = 1.25$ m connected to a standard pressure sensor with an elastance of $K = 3.3 \cdot 10^{14} \frac{\text{Pa}}{\text{m}^3}$, the theoretical natural frequency is estimated at ($f_0 = 48$ Hz) [1].

$$f_0 = \frac{1}{2\pi}\sqrt{\frac{k}{m}} = \frac{r_i}{2}\sqrt{\frac{K}{\pi\rho l}} \tag{3}$$

Volume-restricted areas (e.g., brain or miniature blood vessels) demand thin catheters. Ultra-thin catheters (*i.e.*, microtubing, Johnson Matthey) have an o.d. of 0.3 mm and an i.d. of 0.254 mm (*i.e.*, P.N.24468A) [48]. Replacing the previously mentioned catheter with the ultra-thin catheter ($r_{i2} = \frac{1}{3} r_i$) and assuming the same length, the natural frequency would decrease to $f_{02} = \frac{1}{9} f_0$ (*i.e.*, $f_{02} = 5.3$ Hz). Considering the presence of additional compressible air-bubbles trapped in the catheter structure, damping and reducing the natural frequency [49], it is necessary to locate the sensor at the tip of the catheter or at least very close to it. In the case of very small catheters (below 1 Fr), catheter-tip sensors, such as optical fibres, can uniquely fulfil these requirements.

2.3. Commercial Sensors

The specifications of some commercially available electrical sensors [50–53], which are currently used in medicine, are included in Table 3. Recently, the FDA approved the first implantable wireless sensor for pulmonary artery pressure measurements [54], by CardioMEMS$^{\text{TM}}$.

Table 3. Electrical pressure sensors available on the market.

Company	**Merit Sensor**	**Elcam Medical**	**MEMSCAP**	**Me. Specialities**
Sensor Name	BP series [50]	Sense-IT [51]	SP854 [52]	1620 [53]
Min. Pressure	–4 kPa (–30 mmHg)	–4 kPa (–30 mmHg)	–80 kPa (–600 mmHg)	6.66 kPa (50 mmHg)
Max. Pressure	40 kPa (300 mmHg)	40 kPa (300 mmHg)	93 kPa (700 mmHg)	40 kPa (300 mmHg)
Over Pressure	862 kPa (125 Psi)	862 kPa (6465 mmHg)	1.3 MPa (10 MHg)	862 kPa (125 Psi)
Frequency	1.2 kHz	1.2 kHz	300 Hz	1.2k Hz
Drift	0.125 mmHg·h^{-1}	0.125 mmHg·h^{-1}	-	0.25 mmHg·h^{-1}
Compliant	AAMI, RoHS	510(k), AAMI, CE, ISO 2009, 10993-1	OEM-Part	AAMI, RoHS

Restriction of Hazardous Substances (RoHS); Original equipment manufacturer (OEM); Measurement (Me.) Specialities.

3. Optical Fibre Pressure Sensors

From the 1960s to the early 21st century, optical fibre sensors were largely based on intensity modulation, and this was the dominant technology for use in OFS, at the time being based on a simple architecture and low-cost interrogation. They therefore represented a potential alternative to the standard medical pressure sensors [55].

3.1. The Development of Optical Fibre Sensors

Many early-stage OFSs were based on optical fibre bundles [56,57], which were implemented in a single fibre oriented to a distal reflective mirror [58,59], with a two (or more)-fibre system [60] or a fibre modulated by an internal cavity [61]. Several patents regarding intensity-modulated OFSs were filed from the 1990s onward [62–65], complementing existing patents for catheters to host such sensors, such as Purdy *et al*. [66]. The Camino sensor, industrialized by Integra LifeSciences, represents an important commercially available product and is currently a standard system for the measurement of intra-cranial pressure (ICP) [67–69]. OFS based on a microbending principle (*i.e.*, attenuation of intensity) [70,71] were recently adopted in the pressure measurement area. Intensity-modulated OFS are relatively simple in design and, hence, relatively low cost, but suffer from long-term instability. Changes, such as the variation of the received optical intensity due to source output power drifts, fibre movements, or the degradation (*i.e.*, ageing) of components in the system, or on the fibre tip contribute to error in the measured pressure signal.

Following the advent of the fibre Bragg grating (FBG) sensors (in the 1990s), much research effort was dedicated to applying the emerging FBG technologies to pressure sensing in the medical environment. FBGs are highly sensitive to strain, and due to recent developments in draw-tower

fabrication techniques [72,73] can be manufactured as bend-insensitive fibre structures with excellent tensile strength, on standard 125-µm diameter, as well as 80-µm fibres. A major technical challenge of implementing FBGs as pressure sensors is the physical conversion from pressure to strain, which is the fundamental parameter measured by the FBG. FBG sensing systems are capable of providing a solution to the problem of intensity-modulated OFS, as they provide intensity-independent output.

Within the last seven years, due mainly to improvements in microfabrication technologies (e.g., the availability of splicers, lasers and hybrid electro/optic facilities for optical fibres), cavity structures based on Fabry–Perot principles have become realisable and represent a major research focus in pressure sensing technology. In this context, the Extrinsic Fabry–Perot interferometer (EFPI) represents a significant technological advancement and is based on a sound principle of operation, which is a wavelength-dependent intensity variation resulting in a spectral shift [74]. EFPI sensors have overcome the main drawbacks of intensity-modulated OFS and FBG sensors, in so far as they provide intensity-independent detection, but sensitivity and accuracy are more than three orders of magnitude greater than FBGs.

3.2. Advantages of Optical Fibre Sensors

Sensors based on optical fibres are emerging as an excellent alternative to electrical sensors based on catheters, guidewires and MEMS [75]. For medical applications, OFS have many strategic advantages over classical measurement techniques:

Footprint and geometry: Silica glass-based optical fibres used in most sensors are very small, since they have a 125-µm diameter (e.g., SMF-28 fibres), and optical fibres of an 80-µm diameter are currently commercially available. Furthermore, recently developed draw-tower fabrication of fibres and sensors [76] now allows the fabrication of in-fibre sensors without removing the fibre coating and, therefore, maintaining the tensile strength of the buffered fibre, which is critical when being placed in a range of environments. In addition, the broad availability of bend-insensitive fibres allows the operation of these sensors, even in the presence of tight bending. Commercial catheters have typically 4–6 Fr diameters (1 Fr = $\frac{1}{3}$ mm), where a plurality of optical fibre pressure sensors can fit inside an individual catheter or guidewire.

Distribution and integration: OFS enable the detection of physical parameters (strain, temperature) at several points along a single fibre. This arrangement is extremely common with FBG sensors, using a wavelength division multiplexing (WDM) approach [76–80]. Recently, distributed sensing systems based on Rayleigh backscattering demodulation [81,82] have achieved a spatial resolution better than 1 mm. In addition, with a WDM approach, it is possible to integrate on the same fibre, at the sensing point, a plurality of sensors: a popular arrangement involves the integration of pressure and temperature sensor on the same fibre tip [83–86].

Long-term capabilities: As one of the main trends in biomedical science is to perform long-term diagnostics with minimally-invasive devices, the stability of pressure recording in the long term needs to be guaranteed. OFS guarantee an excellent stability rate, achieving typical stability of 1 $\frac{\text{mmHg}}{\text{hour}}$ with sensor prototypes [87] and about 3 mmHg/28 days in commercial sensors [88].

Thermal properties: The accuracy of pressure sensing technologies is also limited by cross-sensitivity to temperature variations. In the case of many sensors (e.g., electronic, mechanical), a temperature change has a non-linear effect on the output, which can only be mitigated by thermally-insensitive packages. In OFS, however, temperature and pressure dependences are both linear and can be mutually compensated [83].

Total immunity to external EMI: OFS can be fabricated from silica glass, which is a dielectric material and is inherently immune to electromagnetic interference (EMI). This makes OFS-based device compatible with the medical environment where EMI is central to a range of diagnostic and treatment techniques, such as as MRI, computed tomography (CT) scan, RF/microwave thermal ablation and other imaging and invasive medical procedures [70,89].

3.3. Theory and Working Principles

For the medical field, OFS can be grouped according to: (1) the placement area of the sensor (e.g., *in vivo*, *ex vivo*, *in vitro*); (2) the amount of usage (*i.e.*, disposal or reusable); or (3) the pressure range being recorded (low, middle, high). From a technical point, the OFS may be grouped according to structure, modulation and measurement.

The structure of an OFS (Figure 3a) can be divided into intrinsic (*i.e.*, the sensing element is inside of the fibre) or extrinsic (*i.e.*, the fibre is extended with an external sensing element). It also shows the set-up with broadband light source (BLS), which emits a continuous spectrum (1) to the sensing element. There, the signal is modulated (2) by the measurand and travels back though a 3-dB coupler to the optical spectrum analyser (OSA). The advantages of reflection mode (as shown in Figure 3a) as opposed to transmission are that the sensor may be used as a reflective probe and the tip of the sensor can be inserted into the patient.

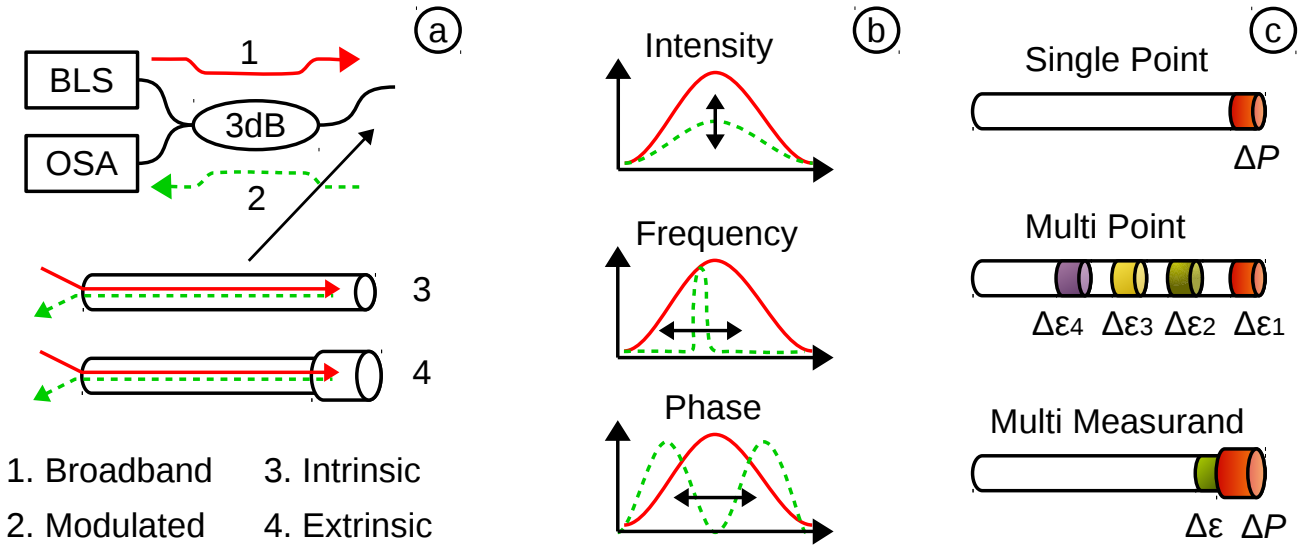

Figure 3. (**a**) The full sensor system based on a broadband light source (BLS), an optical spectrum analyser (OSA) and an intrinsic or extrinsic sensor; (**b**) the signal can be modulated by a change in intensity, frequency or phase; (**c**) the sensor may measure in a single or multi-point and acquire single or multiple measurands.

The modulation for OFPS (Figure 3b) may change: (i) the received intensity (*i.e.*, amplitude of the electric field E) by a displacement of a reflecting surface (e.g., diaphragm) or a bending of a fibre (*i.e.*, attenuation); (ii) the frequency (*i.e.*, wavelength λ) by a change of a the period of the grating (FBG); or (iii) based on a phase modulation (ϕ) (*i.e.*, interferometry by Mach Zehnder, Michelson [90,91] or Fabry–Perot [92]) using the phase property of the light.

The measurement for an OFS (Figure 3c) can depend on: (i) the point of interest (*i.e.*, single point, multi-point or distributed sensing); or (ii) the measurand itself (e.g., pressure (P), temperature (T) or both). It is also possible to extend the OFS to measure other measurands (e.g., from strain (ϵ) to pressure (P)).

3.4. Fabry–Perot Interferometer and Fibre Bragg Grating

The remit of this paper is a review of OFPS based on EFPI and FBG techniques. A more comprehensive review of optical fibre intensity-modulated sensors is available in Roriz *et al.* [55]. A recent review of medical FBG sensors is available in Mishra *et al.* [93] and for Fabry–Perot interferometer (FPI) sensors from Roriz *et al.* [94]. Both sensor types are based on the same principles shown in Equation (1) for the strain gauge and Equation (2) for the diaphragm displacement and can be used both directly and indirectly to measure the pressure. The recently investigated OFPS highlighted in this review are based on both principles and represent a major step forward in the current state of the art.

The Fabry–Perot interferometer is based on the principle of interferometry [92,95]. The Fabry–Perot (FP) cavity is usually located on the tip of an optical fibre and enclosed by a miniature glass diaphragm [74]. The light from the source is coherent in the vicinity of the sensor and can potentially interfere with itself, e.g., by reflection. For a low finesse interferometer (Figure 4a), approximately 4% of the light intensity is reflected at the end face of the single-mode fibre (SMF). The residual light travels the length (L) to the diaphragm, where upon it is also reflected (e.g., another 4% for a glass diaphragm), travels back the same way and finally penetrates back into the SMF. Since the light from the diaphragm has experienced an additional path length ($2L$) through the cavity filled with air (refractive index (n_0)), it has a phase difference, given by Φ_0. The intensity (I) in the spectrum for each wavelength (λ) therefore depends on the distance of the diaphragm (L) to the SMF, shown in Equation (4) [96]. The change of the diaphragm with reference to the pressure (*i.e.*, $\Delta L(\Delta P)$), can be calculated in the same way as previously demonstrated in Equation (2).

$$I(\lambda) = I_1 + I_2 + 2\sqrt{I_1 I_2} \cdot \cos\left(\frac{4\pi \cdot L \cdot n_0}{\lambda} + \Phi_0\right) \tag{4}$$

Alternative solutions for a diaphragm make use of bendable organic material to increase the sensitivity [97], ultra-thin metal diaphragms to improve the reflectivity [98] and a graphene membrane [99], as well as a polymer diaphragm sealed with a ultra violet (UV) mould [84]. Bremer *et al.* [83] demonstrated an EFPI sensors with an integrated FBG sensor for dual pressure/temperature detection and mutual compensation. Bae *et al.* [100] in fact proposed a multi-cavity approach for dual sensing. Their high sensitivity and accuracy, as well as their dual sensing versatility have resulted in commercial systems based on EFPI technology gaining momentum and an increasing market share [88,101,102].

The fibre Bragg grating is formed as a periodic change of the refractive index n_{co} (the core refractive index) with a distance of Λ (the pitch of the grating). The light is partially reflected at each grating period. This results in a narrow-band reflection at the Bragg wavelength (λ_B), as shown in Equation (5), where n_{eff} is the effective refractive index of the optical fibres core in the region of the grating. With applied strain (ϵ), the pitch of the grating changes and, therefore, the Bragg-wavelength.

$$\lambda_B = 2n_{eff} \cdot \Lambda \tag{5}$$

The challenge is to measure the pressure and convert it into mechanical strain, so that it may be measured by the FBG. Kanellos *et al.* proposed a pressure sensor based on four FBGs based on a flexible patch [103]. Ahmad *et al.* [104] proposed a similar form factor. Another working principle proposed by Zhang *et al.* [105] was based on a piston-like architecture. FBG-based sensors are also gathering significant traction in novel robotic micro-surgery systems [106,107] for the measurement of axial and lateral contact force.

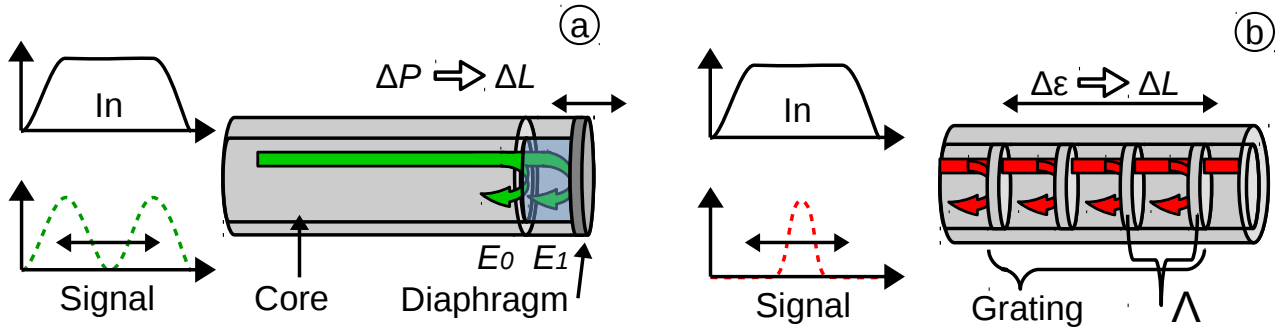

Figure 4. Reflected light in: (**a**) a low finesse Fabry–Perot interferometer (FPI) sensor and (**b**) in a FBG sensor.

4. Optical Fibre Pressure Sensors in Medicine

Optical fibre sensors have been proposed for biomedical applications (e.g., *in vivo*, *ex vivo* or *in vitro*) for several decades. Early investigations of *in vivo* applications were undertaken [108], and many reviews have recently been compiled to evaluate their advantages in the medical field [109–115]. It is therefore the role of this review to highlight the use of optical fibre pressure sensors in the state-of-the-art medical practice.

4.1. Introduction

Lindström [59] proposed the first medical optical fibre pressure sensor in 1970. In 1984, Peterson and Vurek [116] analysed the utilisation of optical fibres. Nowadays, optical fibres can be fabricated from a wide range of different materials (e.g., plastic, chalcogenide glass), whereas silica glass-based fibres are known to have good bio-compatibility. Hench and Wilson [117] initially reviewed the compatibility of silica in 1986. This study was extended for silica-based MEMS [118,119] and finally tested for long-term *in vivo* implantation [120,121]. Yang *et al.* [122] (2003) tested OFS-based pressure sensors for 12 weeks and demonstrated their bio-compatibility and usability for *in vivo* human applications.

As previously outlined, modern optical fibre sensing technologies provide many advantages over non-OFS technologies when used for medical application. Their small size (Figure 5) makes them ideal for use in volume-restricted areas. Since they are fabricated from silica glass, they are immune to RF and, therefore, compatible for use in MRI. OFS (a Furukawa company) offers bio-compatible fibres for medical application. These fibres are bend resistant and also offer bio-compatible coatings, certified by North American Science Associates, Inc. (NAMSA) with ISO 10993 [123]. Optical sensors can also be sterilized, without affecting their properties. Stolov *et al*. [124] demonstrated the possibility of: (i) steam sterilization; (ii) ethylene oxide and (iii) gamma radiation on optical fibres with: (1) dual acrylate; (2) polyimide; (3) silicone polyether ether ketone (PEEK); and (4) fluoroacrylate hard cladding ethylene tetrafluoroethylene (ETFE).

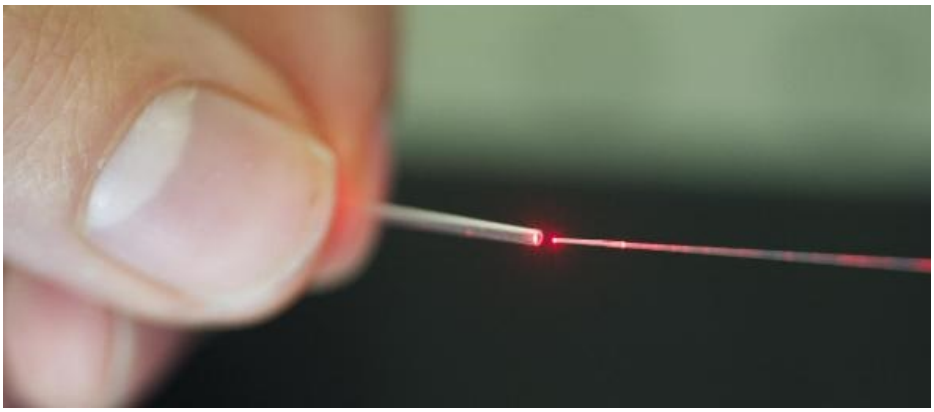

Figure 5. OFPS (**right**) illuminated in red and placed into a miniaturized catheter (**left**).

4.2. Research on Medical Optical Pressure Sensors: In Vivo

In this review, OFPS are presented, which are used in the medical field for both *in vivo* and *ex vivo* applications as outlined in the literature. In some cases, the available literature is minimal; in other cases, there is extensive and detailed information available on the relevant sensors. Some typical medical application areas are highlighted below in which the use of OFS has proven successful.

Gastroenterology: 60–70 million Americans are affected by Gastrointestinal conditions every year [125]. One of the most common gastrointestinal symptoms is abdominal pain, which results in hospitalization in 15.9 million cases [126]. The magnitude of this medical condition and the implications for the health economy dictate the need for an inexpensive method of investigating the gastrointestinal tract.

In 2007, Takeuchi *et al*. [127] published a study on pharyngeal manometry. They used an FPI-based pharyngeal manometric sensor for deglutition analysis. The sensor (FOP-MIV, FISO Technologies) showed good agreement with their catheter-type reference sensor (P37-4109C05, Zinetics). The whole catheter structure was of a small size of only 2.08 mm in diameter, covering a pressure range of 30 kPa–30 kPa and a sampling frequency of 250 Hz. The sensor demonstrated a correlation factor of 0.999 to the reference sensor, and furthermore, a trace of a period of *in vivo* swallowing processes was recorded online and demonstrated good agreement with the reference instruments. The same sensor type

(FOP-F125, FISO) was used by Kong *et al*. [128] (2013) for oesophageal variceal pressure measurements in three different patients.

Arkwright *et al*. [129,130] (2009) presented a manometry catheter based on FBG arrays (from FBGs) with a series of 72 sensing elements with a spacial distance of 1 cm. Each FBG is inserted into a casing design (schematic in Figure 6a) and is used to transpose pressure into strain, resulting in multi-pressure measurements [131,132]. The sensor structure was tested for 0–26.7 kPa (0–200 mmHg) with an accuracy of 0.4 kPa (3.1 mmHg), a sensitivity of –0.001 $\frac{\text{nm}}{\text{mmHg}}$ and a frequency of 10 Hz. The FBGs are surrounded by a transducer, converting the pressure into strain (Figure 6a). The catheter (Figure 6b) was tested *in vivo* in a human colon over 24 h. In their study, they placed the sensing elements in the ascending colon, in the transverse colon, in the descending colon and in the sigmoid colon [129]. This successful test revealed the complex pressure nature of the colon for the first time. This technique is an example of where optical fibres have surpassed the gold-standard and, in fact, opened a new area of high-resolution manometry (HRM). This technique was recently (2014) used in a study of 10 healthy humans and revealed a new understanding in the propagating motor pattern of the human colon [133].

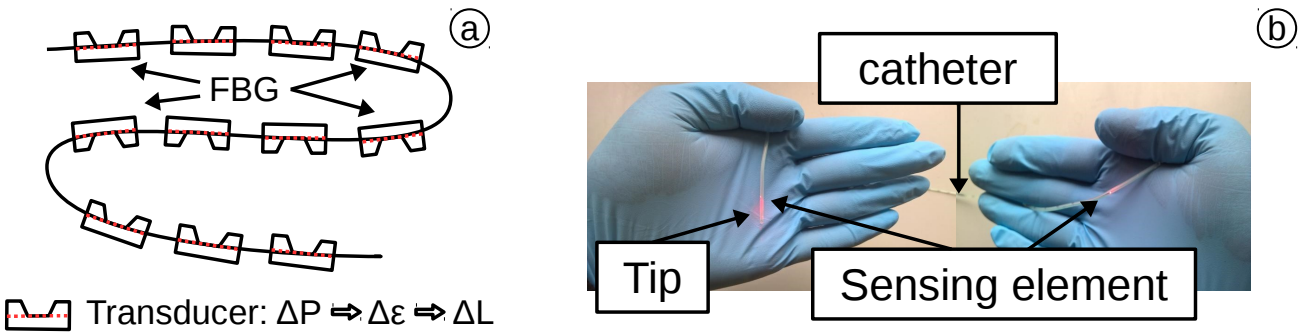

Figure 6. (**a**) Distributed pressure sensor based on an FBG chain with transducers; (**b**) sensor placed in a catheter.

Cardiology: The recent report (2014/2015) of the American Heart Association (AHA) [134,135] revealed that in 2011, *ca*. 600,000 Americans died as a result of heart disease with a cost (direct and indirect) of 215.6 billion $. This again demonstrates the need to introduce cost saving methods within the healthcare system without compromising the quality of patient care.

The first optical sensor for intra-vascular pressure measurement was developed and clinically tested by Lindström *et al*. [59] in 1970. This intensity-based sensor was instrumental in optical sensors achieving successful entry into medicine. In 2002, Reesink *et al*. [136] published a feasibility study, using fibre-optic systems (Model 40EC, RJC enterprise) for invasive blood pressure measurements. They compared the OFPS *in vitro* to the gold-standard Millar (SPC-320 with a bridge amplifier), Baxter (uniflow external pressure transducer) and Sentron devices. Further tests *in vivo* in two goats followed. They demonstrated the high similarity of the OFPS to these gold-standard sensors. In 2003, Woldbaek *et al*. [137] described the use of an OFPS for pressure recording in the cardiology setting. They used an optical sensor (Samba) for pressure measurements in mice. They tested the sensors (o.d. 0.42 mm) *in vitro* with a drift of <60 $\frac{\text{Pa}}{\text{h}}$ (<0.45 $\frac{\text{mmHg}}{\text{h}}$) and a temperature sensitivity of only ∼9 $\frac{\text{Pa}}{\text{k}}$ (∼0.07 $\frac{\text{mmHg}}{\text{k}}$) in the range of 22–37 °C. With a frequency response of 0–200 Hz, this sensor fulfils the technical specification. They inserted the OFPS in 18 male mice, into the left carotid artery to measure

the aortic pressure (AP) and heart rate continuously. The optical sensor demonstrated good functionality, and Woldbaek *et al*. [137] concluded that this sensor is suitable for blood pressure measurement, even in small vessels.

Schreuder *et al*. [138] (2005) published a new measurement method using automatic intra-aortic balloon pumping (IABP) with a dicrotic notch prediction algorithm. For their evaluation, they applied an optical sensor (they refer to the same one that Reesink *et al*. used) in 27 patients with low ejection fraction (*i.e.*, undergoing cardiac surgery) for 20–48 h. The optical fibre sensor, combined with their novel algorithm, allowed a fully-automatic IABP timing. In the same year (2005), Pinet *et al*. [139] proposed that their OFPS (FISO) based on a micro-optical mechanical systems (MOMS) could also be used for IABP. A detailed analysis of the effect of fibre-optic IABP therapy on clinical management was performed by Yarham *et al*. [140]. Their FOP-MIV is now also FDA approved. Furthermore, a patent for an intra-aortic balloon catheter with a dual pressure sensor technology was filed in 2007 [141]. Mulholland *et al*. [142] (2012) reported the insertion of an 8-Fr, 50-cc SensationPlus^{TM} intra-aortic balloon (IAB) catheter (Maquet Cardiocascular) in a 53-year-old man. As a result, the catheter expands the patients vessel, which results in greater diastolic blood volume, and the sensor supported more accurate monitoring.

Wu *et al*. [143] (2013) developed an optical sensor and used it in conjunction with a fractional flow reserve (FFR) technique in a swine model. In the last two years (2014–2015), the amount of research in this field has rapidly increased [144–148]. In 2014, Rodriguez *et al*. [149,150] used an OFPS (OPP-M, Opsens) for simultaneous pressure and volume measurement. The immunity to electromagnetic fields made it possible to use the sensor in an MRI during a left ventricle function assessment while undertaking an *in vivo* experiment in a ewe. The results were compared to the Millar sensor and demonstrated good correlation.

Neurology: A significant increase in ICP can be life threatening for neurological patients [151]. This can be caused by disease (e.g., cancer growth or accumulation of blood) or factors, such as blasts from explosions (e.g., improvised explosive devices (IEDs)). To confirm raised intra-cranial pressure, optical fibres can play a decisive role.

In 1996, Shapiro *et al*. [152] demonstrated intra-parenchymal cerebral pressure monitoring in 244 patients (e.g., with intra-cerebral pathology, including trauma and intra-cerebral haemorrhage), using OFS technology. The measurements were performed from 1988–1993 with an average time of seven days (up to 24 days) of observation. Only one patient acquired an infection, and in this case, the infection developed towards the end of the observation period of 23 days. The OFPS (Model 110-4B, Camino Laboratories) was housed in a catheter and was inserted via a hole drilled in the skull and closed by a locking screw (schematic in Figure 7a). This study demonstrated easy and safe monitoring of ICP. In 2007, Bekar *et al*. [153] published an analysis of the risk factors of OFPS in intra-cranial pressure monitoring on 631 patients. They concluded that the ICP monitoring system could be safely used and that the infection risk is low (1.8%).

Chavko *et al*. [154] (2007) demonstrated an intra-cranial pressure measurement in generated blast waves using OFPS. The sensors were placed in the third cerebral ventricle of anaesthetized male rats. The pressures recorded were as high as 40 kPa and measured for several milliseconds. The rats were placed in pneumatic-driven shock tubes (schematic in Figure 7b), generating the blast waves. A

1 mm hole was drilled into the head of the rats, and the sensor, placed in a 23-gauge catheter, was inserted. Leonardi *et al*. [155,156] tested with the same sensor (FOP-MIV) and a similar experimental configuration the ICP of 25 rats.

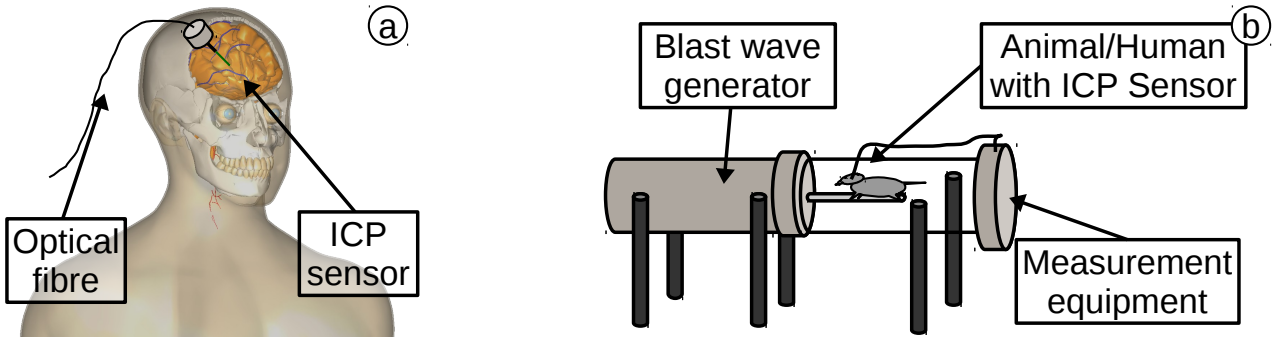

Figure 7. (**a**) ICP sensor, inserted into brain (created in bodyparts3d [13,14]); (**b**) schematic of blast wave generator with animal and ICP sensor inside.

An analysis of the transient response in a human skull, with exposure to blast waves, was published by Bir [157] in 2011. The shock waves produced a pressure up to 137.9 kPa. The OFPS (FOP-MIV, FISO) was placed in frozen human heads and placed in the tube. During 15 blast simulations, the sensors measured the pressure in four different areas of the brain. The experiments demonstrated the importance of sensor location, the intensity of the blast wave and the orientation of the head to the wave when undertaking sensor measurements in the brain.

Urodynamics: The pressure measurements undertaken during the course of urodynamic studies and which are relevant to the lower urinary tract (LUT) requires measurement in the urethra, bladder and abdomen. This analysis is important in order to diagnose bladder-related conditions [28,158]. Urodynamic analysis plays a key role as a method to localise pathological obstruction [159].

In 1993, Belville *et al*. [160] demonstrated the feasibility of a urodynamic system with OFPS (FST 200). The optical sensor was placed in a 1.6-mm (5 Fr) catheter, which was FDA approved for multiple usage. The sensor was based [160] on a diaphragm displacement technique with an intensity-modulated signal. The properties of the system demand a calibration cycle of 15 s before each use. The resolution in pressures measured was better than 100 Pa (1 cm H_2O) up to a frequency of 50 Hz.

Poeggel *et al*. [87] (2014) achieved *in vivo* bladder and abdominal measurements in patients, using a differential measurement technique, which allowed the simultaneous measurement of urodynamic pressure in a 1.6-mm (5 Fr) catheter, as well as abdominal pressure (Figure 8a,b). In a study published in 2015 [161] (Figure 8c), the technique was extended using an EFPI sensor with integrated FBG (*i.e.*, measuring pressure and temperature with a single sensor), creating an optical fibre pressure and temperature sensor (OFPTS). Furthermore, two sensors were placed in a single 1.6-mm (5 Fr) catheter, with a separation of 1 cm. This technique facilitated a true differential pressure measurement.

Additional *in vivo* pressure measurements were undertaken in humans and animals. Some of them are listed here, in order to demonstrate the range of use of optical fibre pressure sensors. These include measurements of intra-cochlear pressure (ear pressure) [162], dental pressure [163,164], intra-ocular pressure (IOP) [165,166] or vitreoretinal microsurgery [167,168].

A sensor for the dynamic assessment of the female pelvic floor function by intra-vaginal pressure was developed by Ferreira *et al.* [169]. The sensor (based on an FBG) was inserted into a silicon probe that measured radial muscle pressure and used this to interpret the axial load. The intra-abdominal pressure (IAP) of the glenohumeral joint was analysed by Inokuchi *et al.* [170]. The intra-muscular pressure (IMP) in rats was measured by Cottler *et al.* [171] and in the legs of four female and three male humans by Nilsson *et al.* [172]. Le *et al.* [173] developed a pressure sensor for tissue. In 2015, Roritz *et al.* [174] measured the pressure in the intervertebral disc pressure (IDP) of an anaesthetized sheep. The intra-discal pressure pattern was measured in the fifth lumbar disc, and this showed good agreement with previous results during spontaneous breathing. Furthermore, the lung pressure was measured in a different set of experiments. An OFPS (Camino 420 XP) was used in the endotracheal tube by De Blast *et al.* [175]. Intra-tracheal pressure was measured by Sondergaard *et al.* [176] and intra-oesophageal pressure by Hogan and Mintchev [177].

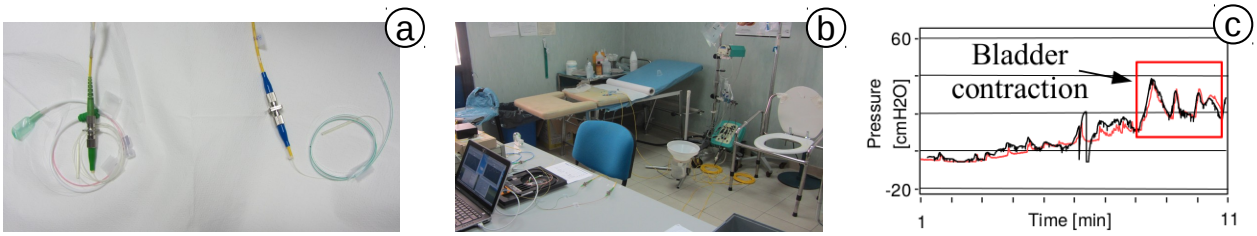

Figure 8. (**a**) Left: abdominal balloon catheter; right: bladder catheter; (**b**) examination chair with equipment; (**c**) urodynamic measurement.

4.3. Research in Medical Optical Pressure Sensors: Ex Vivo

Ex vivo pressure measurements are measured outside of the body, disembowelled organs or in phantoms. The restrictions applied to these measurements are not as rigorous as for *in vivo* in humans or animals. Some recent experiments in this area are described below.

Thermal ablation is an invasive hyperthermia procedure: using a radio-frequency, microwave, laser or ultrasound source, using a micro-miniature applicator, delivered to the precise point of treatment. Using this technology, it is possible to generate a heat field *in vivo* with excellent localization capability. The radio frequency ablation (RFA) therefore has been successfully applied to many recent cancer treatments [178,179]. Using a percutaneous miniature applicator, RFA induces a heat field in excess of 3 °C/mm at the point of treatment. Cancer cells are euthanized as a function of temperature and the duration of its exposure [180].

Due to the lack of suitably-miniature and electrically-immune measurement equipment, it is not possible to implement pressure measurement in clinical RFA. The first pressure experiment in RFA is credited to Kotoh *et al.* [181] (2005), using an MEMS sensor positioned 3 cm from the ablation point. Previously, it was not possible to incorporate pressure sensing in the delivery of radio-frequency ablation due to the lack of a suitable sensing system.

Tosi *et al.* [86] (2014) performed the first pressure measurement *ex vivo* for RFA, with an OFPTS (Figure 9a) implementing a sensor on an animal liver phantom (Figure 9b). The sensing system used

has the key advantage of having low thermal sensitivity, which allows operation at the point of ablation without the negative effects of large temporal and spatial temperature variations. A methodology for pressure measurement in RFA is reported in [182]. Pressure was recorded as 162 kPa (at 164 °C temperature), while in [86], a peak value of 750 kPa was recorded due to the encapsulation of the phantom (Figure 9c).

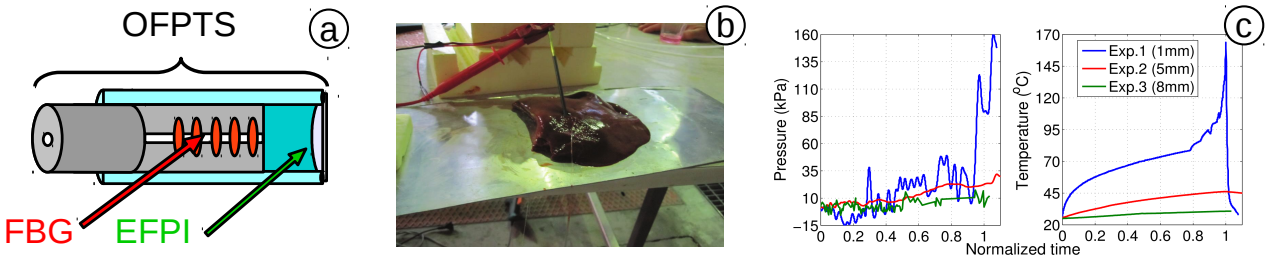

Figure 9. (**a**) OFPTS with EFPI and integrated FBG sensing element [183]; (**b**) liver phantom with OFPTS; and (**c**) pressure and temperature distribution in time. (adapted from Figures 21a and 24: Tosi, D., licensed under CC Attribution-Adapt Alike 3.0, 2015 [182])

Additional *ex vivo* measurements of heart rate were recorded using optical fibre macro bending sensors on foot artery [184] or mounted around the arm [185]. FPI sensors for needle tip force sensing were tested on a medical skin phantom [186]. An *ex vivo* pressure test was also performed in lumbar IDP [187]. Smart devices have also been developed, where FBGs were inserted in clothes [188], beds [189,190] or furniture [191]. A wide variety of *ex vivo* or *in vitro* pressure measurements in other physiological locations have been successfully performed, including oesophageal pressure [192] and lung pressure during respiration [193].

4.4. Optical Pressure Sensors: Companies and Products

Companies that offer optical sensors [88,101,102,194–196] are listed in Table 4, demonstrating their potential for medical application [61,127,136,142,149,155,166,197–207].

5. Conclusions

The purpose of this review was to provide an update of the current state-of-the-art in optical fibre pressure sensors (OFPS) for use in the medical field. The sensors highlighted in this review are based on the principles of a Fabry–Perot interferometer (FPI) and fibre Bragg grating (FBG) techniques, whose characteristics and performance (e.g., range, sensitivity) are comparable, if not superior to commercially available electronic pressure sensors. However, instead of an electrical signal, the sensors modulate light. The absence of electrical signals makes the optical fibre sensors immune to radio frequency (RF) signals, which offer unique benefits, e.g., in harsh environments, such as MRI. The small diameter makes the sensor suitable for medical applications in volume-restricted areas, such as blood vessels or internal organs. The low attenuation of the optical single mode fibre (SMF) allows a potentially very long distance from the sensing element to the acquisition system, which is an advantage, e.g., in dangerous conditions, such as an epidemic patient in a contamination room without adequate equipment.

Additionally, if a pressure sensor system were brought into such an area, it could be hard to remove, exchange or repair the system without taking additional risk. Furthermore, OFPS are inexpensive to produce, which makes them easily disposable. This may reduce the risk of infection, and since they are fabricated from glass, a disposable sensor has less impact on the environment when disposal is required. These above properties of OFS represent significant advantages, compared to electrical sensors, which makes them particularly well suited for medical application.

Furthermore, the human organism is a complex combination of a variety of organs, bones, joints and muscles, all of which have different pressure properties and measurement requirements. These requirements are often defined in standards, which are approved by authorizing institutions, such as FDA and ISO. Therefore, any optical sensor system has to be adapted to the needs of the specific medical examination. The sensitivity of FPI sensors can be easily adjusted by changing the thickness, material and diameter of the diaphragm. The change of sensitivity, as the main factor for determining pressure resolution, allows the adoption of the same sensor design for use in high-range or high-resolution sensors. With the inclusion of FBGs, it is possible to achieve single (e.g., for pressure and temperature) or multi-point measurements in a single 125–200-μm sensing element. OFPS have demonstrated stabilities up to 3 mmHg/23 days, which also allow accurate long-term measurements, which due to their size, can be fully *in vivo*. Their small size also allows the sensors to be placed in a standard catheter and, hence, for it to be guided to the point of interest, which avoids the use of over-/under-damping of water/air-filled catheters and gives a more accurate pressure signal.

Nevertheless, a high variety of *in vivo* and *ex vivo* applications have already been demonstrated and reviewed in this article. Optical pressure sensors for ICP and IABP have become the norm for clinical use in recent years. Furthermore, new technologies, such as the multipoint manometry catheter, based on an FBG array with up to 72 sensing elements, have the potential to create new gold standards. The small size allows housing of dual (or multiple) sensors in one catheter, which allows differential analysis as demonstrated in urodynamic measurements. Additionally, newer technologies, such as a radio-frequency RF ablation technology, have shown how optical fibre-based pressure sensors can satisfy modern medical demands, which other sensor technologies are not able to do. A summary of the main research impact, based on the number of publications, is included in Table 5. It demonstrates the current state of sensor technologies, how far the medical field of OFPS has penetrated into this application area, as well as the research impact. In particular, the latest test results captured in real medical environments demonstrate the excellent potential for future clinical use and emerging application areas for OFPS.

Table 4. Optical pressure sensors available on the market.

Company	**Samba**	**FISO**	**Camino**	**Opsens**	**RJC Enterprise**	**Maquet**
Sensor Name	Preclin 420/360 Transducer [194]	FOP-MIV (R1) [101]	Model 110-4B [195]	OPP-M25 [88]	Model 40 [102]	CS300 [196]
Min. Pressure	–5 kPa (–37.5 mmHg)	–40 kPa (–300 mmHg)	–1.3 kPa (–10 mmHg)	–6.66 kPa (–50 mmHg)	66 kPa (500 mmHg)	0 kPa (0 mmHg)
Max. Pressure	35 kPa (262 mmHg)	40 kPa (300 mmHg)	16.7 kPa (125 mmHg)	40 kPa (300 mmHg)	133 kPa (1000 mmHg)	40 kPa (300 mmHg)
Pr. Resolution	10 Pa (0.07 mmHg)	40 Pa (0.3 mmHg)	-	66 Pa (0.5 mmHg)	< 0.1 mmHg	-
Over Pressure	-	530 kPa (4000 mmHg)	166.7 kPa (1250 mmHg)	533 kPa (4000 mmHg)	-	-
Frequency	40 kHz	250 Hz	120 Hz	250 Hz	1 kHz	26 Hz
Diameter (in Catheter)	0.36–0.42 mm	0.55 mm	1.35 mm (4 Fr)	0.25 mm	0.17 mm	2.33 mm (7 Fr)
Approved	-	FDA	FDA	-	(AAMI BP)	FDA
Tested for	left ventricle [197] ICP [198,199] IDP [200]	IAP *1 [201], pharyngeal *1 [127], ICP [155,202]	ICP *1 [203,204] IMP *1 [61,205] IAP [206]	IAP [149] IOP [166]	AP [136]	IABP *1 [142,207]

In some cases, a different sensor by the same company was used. However, the references demonstrate the feasibility; Measurements in a human are marked with (*1). IDP, intervertebral disc pressure; IAP, intra-articular pressure; IOP, intra-ocular pressure; IABP, intra-aortic balloon pumping; Pr., Pressure.

Table 5. Main publications, sorted by the number of publications in this review.

Medical Area	Modulation Type	Place	Temperature Compensation	Sensor State	Already Explored	Research Impact	Publications
Cardiology	Intensity, FPI, FBG	*in vivo*, *ex vivo*	No	100 % *1	70 %	70 %	18
Neurology	Intensity, FPI	*in vivo*	No	100 % *1	70 %	60 %	9
Gastroenterology	FPI, FBG	*in vivo*	Possible	70 %	50 %	60 %	7
Pulmonology	Intensity	*in vivo*, *ex vivo*	No	30 %	20 %	20 %	4
Ophthalmology	FPI, FBG	*ex vivo*	No	40 %	20 %	30 %	4
Urology	Intensity, FPI + FBG	*in vivo*	Yes	60 %	30 %	40 %	3
Rheumatology	Intensity, FBG	*in vivo*, *ex vivo*	No	60 %	30 %	40 %	3
RF ablation	FPI + FBG	*ex vivo*	Yes	30 %	20 %	60 %	2

*1 Medical sensors existing on the market and used by clinicians for medical examinations.

Acknowledgments

This work was supported by the Science Foundation Ireland (10/RFP/ECE2898) and the Irish Research Council (EP-SPG/2011/343).

Conflicts of Interest

The authors declare no conflict of interest.

References

1. Tagawa, T.; Tamura, T.; Oberg, P.A. Pressure Measurement. In *Biomedical Sensors and Instruments*, 2nd ed.; CRC Press: Boca Raton, FL, USA, 2011; Chapter 2.
2. Pollak, J.T.; Neimark, M.; Connor, J.T.; Davila, G.W. Air-Charged and microtransducer urodynamic catheters in the evaluation of urethral function. *Int. Urogynecol. J.* **2004**, *15*, 124–128.
3. Cooper, M.; Fletter, P.; Zaszczurynski, P.; Damaser, M. Comparison of air-charged and water-filled urodynamic pressure measurement catheters. *Neurourol. Urodyn.* **2011**, *30*, 329–334.
4. Digesu, G.A.; Derpapas, A.; Robshaw, P.; Vijaya, G.; Hendricken, C.; Khullar, V. Are the measurements of water-filled and air-charged catheters the same in urodynamics? *Int. Urogynecol. J.* **2014**, *25*, 123–130.
5. Wang, Q.; Brunner, H.R.; Burnier, M. Determination of cardiac contractility in awake unsedated mice with a fluid-filled catheter. *Am. J. Physiol. Heart Circ. Physiol.* **2004**, *286*, H806–H814.
6. Mar, C.E.; Frisbie, J.S. Liquid Filled Low Profile Dilatation Catheter. U.S. Patent 4,793,350, 27 December 1988.

7. Goldstein, B.H.; Fifer, C.G.; Armstrong, A.K.; Gelehrter, S.K.; Treadwell, M.C.; van de Ven, C.; Rocchini, A.P. Use of a pressure guidewire in fetal cardiac intervention for critical aortic stenosis. *Pediatrics* **2011**, *128*, e716–e719.
8. Zampi, J.D.; Hirsch, J.C.; Goldstein, B.H.; Armstrong, A.K. Use of a Pressure Guidewire to Assess Pulmonary Artery Band Adequacy in the Hybrid Stage I Procedure for High-risk Neonates with Hypoplastic Left Heart Syndrome and Variants. *Congenit. Heart Dis.* **2013**, *8*, 149–158.
9. Anderson, K.M.; Brumwell, D.A. Implantable Dynamic Pressure Transducer System. U.S. Patent 4,485,813, 4 December 1984.
10. Ellozy, S.H.; Carroccio, A.; Lookstein, R.A.; Minor, M.E.; Sheahan, C.M.; Juta, J.; Cha, A.; Valenzuela, R.; Addis, M.D.; Jacobs, T.S.; *et al*. First experience in human beings with a permanently implantable intrasac pressure transducer for monitoring endovascular repair of abdominal aortic aneurysms. *J. Vasc. Surg.* **2004**, *40*, 405–412.
11. Abdul Razak, A.H.; Zayegh, A.; Begg, R.K.; Wahab, Y. Foot plantar pressure measurement system: A review. *Sensors* **2012**, *12*, 9884–9912.
12. Belleville, C. Guidewire with Internal Pressure Sensor. U.S. Patent 14/537,417, 10 November 2014.
13. Mitsuhashi, N.; Fujieda, K.; Tamura, T.; Kawamoto, S.; Takagi, T.; Okubo, K. BodyParts3D: 3D structure database for anatomical concepts. *Nucleic Acids Res.* **2009**, *37*, D782–D785.
14. Okubo, K. BodyParts3D. BodyParts3D, by The Database Center for Life Science. Available online: http://lifesciencedb.jp/bp3d/ (accessed on 10 July 2015).
15. Clausen, I.; Glott, T. Development of Clinically Relevant Implantable Pressure Sensors: Perspectives and Challenges. *Sensors* **2014**, *14*, 17686–17702.
16. Food and Drug Administration (FDA). Use of International Standard ISO 10993, Biological Evaluation of Medical Devices Part 1: Evaluation and Testing. Available online: http://www.fda.gov/downloads/medicaldevices/deviceregulationandguidance/guidancedocuments/ucm348890.pdf (accessed on 10 July 2015).
17. International Standardization Organization. ISO 13485:2003 Medical Devices—Quality Management Systems—Requirements for Regulatory Purposes. International Organization for Standardization: Geneva, Switzerland, 2003. Available online: http://www.iso.org/iso/catalogue_detail?csnumber=36786 (accessed on 1 May 2015).
18. International Standardization Organization. Non-Invasive Sphygmomanometers–Part 2: Clinical Validation of Automated Measurement Type. Available online: http://www.iso.org/iso/iso_catalogue/catalogue_ics/catalogue_detail_ics.htm?csnumber=50814 (accessed on 14 July 2015).
19. Date, P. Approved American National Standards. ANSI: Washington, DC, USA, 2015.
20. ANSI/AAMI. *Manual, Electronic or Automated Sphygmomanometers*; Technical Report; ANSI/AAMI: Arlington, VA, USA, 2003.
21. ANSI/AAMI. *ANSI/AAMI BP22: 1994 Blood Pressure Transducers*; Technical Report; AAMI: Arlington, VA, USA, 1994.

22. Chobanian, A.V.; Bakris, G.L.; Black, H.R.; Cushman, W.C.; Green, L.A.; Izzo, J.L., Jr.; Jones, D.W.; Materson, B.J.; Oparil, S.; Wright, J.T., Jr.; *et al*. The seventh report of the joint national committee on prevention, detection, evaluation, and treatment of high blood pressure: The JNC 7 report. *JAMA* **2003**, *289*, 2560–2571.
23. Baura, G. Blood pressure monitors. In *Medical Device Technologies: A Systems Based Overview Using Engineering Standards*; Academic Press: Waltham, MA, USA, 2011; Chapter 7.
24. Hall, J.E. *Guyton and Hall Textbook of Medical Physiology*; Elsevier Health Sciences: Waltham, MA, USA, 2010.
25. Nyquist, H. Certain Topics in Telegraph Transmission Theory. *Trans. Am. Inst. Electr. Eng.* **1928**, *47*, 617–644.
26. Baura, G. Diagnosis and therapy. In *Medical Device Technologies: A Systems Based Overview Using Engineering Standards*; Academic Press: Waltham, MA, USA, 2011; Chapter 1.
27. Gardner, R.M. Direct blood pressure measurement–dynamic response requirements. *Anesthesiology* **1981**, *54*, 227–236.
28. Schäfer, W.; Abrams, P.; Liao, L.; Mattiasson, A.; Pesce, F.; Spangberg, A.; Sterling, A.M.; Zinner, N.R.; Kerrebroeck, P.V. Good urodynamic practices: Uroflowmetry, filling cystometry, and pressure-flow studies. *Neurourol. Urodyn.* **2002**, *21*, 261–274.
29. Griffiths, D.; Hofner, K.; van Mastrigt, R.; Rollema, H.J.; Spangberg, A.; Glaeson, D. Standardization of terminology of lower urinary tract function: Pressure-Flow studies of voiding, urethral resistance, and urethral obstruction. *Neurourol. Urodyn.* **1997**, *16*, 1–18.
30. Rowant, D.; James, E.D.; Kramer, A.E.; Sterling, A.M.; Suhel, P.F. Urodynamic equipment: Technical aspects. *J. Med. Eng. Technol.* **1987**, *11*, 57–64.
31. Abrams, P.; Cardozo, L.; Fall, M.; Griffiths, D.; Rosier, P.; Ulmsten, U.; van Kerrebroeck, P.; Victor, A.; Wein, A. The standardisation of terminology of lower urinary tract function: Report from the standardisation sub-committee of the international continence society. *Am. J. Obstet. Gynecol.* **2002**, *187*, 116–126.
32. ANSI/AAMI. *ANSI/AAMI NS28: 1988 (R2010) Intracranial Pressure Monitoring Device*; Technical Report; ANSI/AAMI/ISO: Arlington, VA, USA, 2010.
33. Andrews, P.J.; Citerio, G.; Longhi, L.; Polderman, K.; Sahuquillo, J.; Vajkoczy, P.; Care, N.I. of the European Society of Intensive Care Medicine, E.M.N.S. NICEM consensus on neurological monitoring in acute neurological disease. *Intensiv. Care Med.* **2008**, *34*, 1362–1370.
34. Frey, U.; Stocks, J.; Coates, A.; Sly, P.; Bates, J. Specifications for equipment used for infant pulmonary function testing. ERS/ATS task force on standards for infant respiratory function testing. European respiratory society/American thoracic society. *Eur. Respir. J.* **2000**, *16*, 731–740.
35. Kharitonov, S.; Alving, K.; Barnes, P. Exhaled and nasal nitric oxide measurements: Recommendations. *Eur. Respir. J.* **1997**, *10*, 1683–1693.
36. Bensenor, F.E.; Vieira, J.E.; Auler, J.O.C., Jr. Guidelines for inspiratory flow setting when measuring the pressure-volume relationship. *Anesth. Analg.* **2003**, *97*, 145–150.
37. Rao, S.S.C.; Azpiroz, F.; Diamant, N.; Enck, P.; Tougas, G.; Wald, A. Minimum standards of anorectal manometry. *Neurogastroenterol. Motil.* **2002**, *14*, 553–559.

38. Coss-Adame, E.; Rao, S.S.; Valestin, J.; Ali-Azamar, A.; Remes-Troche, J.M. Accuracy and Reproducibility of High-definition Anorectal Manometry and Pressure Topography Analyses in Healthy Subjects. *Clin. Gastroenterol. Hepatol.* **2015**, *13*, 1143–1150.
39. Weinreb, R.N.; Brandt, J.D.; Garway-Heath, D.; Medeiros, F. *Intraocular Pressure*; Kugler Publications: Amsterdam, Netherlands, 2007; Volume 4.
40. ISO. *ISO-8612: Ophthalmic Instruments—Tonometers*; International Organization for Standardization: Geneva, Switzerland, 2009.
41. ISO. *ISO-14242-2: Implants for Surgery—Wear of Total Hip-Joint Prostheses—Part 2: Methods of Measurement*; International Organization for Standardization: Geneva, Switzerland, 2000.
42. National Honor Society (NHS). *Buyers Guide-Urodynamic Systems-CEP08045*; Technical Report; NHS Purchasing and Supply Agency: Pittsburgh, PA, USA, 2008.
43. Wilson, J.S. Pressure measurement: Principles and practice. *Sensors* **2003**, *20*, 19–37.
44. Swanson, R.H. *A Low-Cost Instrument to Measure Temperature or Resistance Accurately*; Rocky Mountain Forest and Range Experiment Station, Forest Service, US Department of Agriculture: Washington, DC, USA, 1967; Volume 80.
45. Stefanescu, D. Wheatstone Bridge—The Basic Circuit for Strain Gauge Force Transducers. In *Handbook of Force Transducers*; Springer: Berlin/Heidelberg, Germany, 2011; pp. 347–360.
46. Ahn, W.; Bahk, J.H.; Lim, Y.J. The "gauge" system for the medical use. *Anesth. Analg.* **2002**, *95*, doi:10.1213/00000539-200210000-00076.
47. Kucklick, T.R. *The Medical Device R&D Handbook*; CRC Press: Boca Raton, FL, USA, 2012.
48. Components, J.M.M. *Precious Metals—Tubing*; Technical Report; Johnson Matthey Medical Components: West Chester, IL, USA, 2015.
49. Weisz, M.; Johnston, V. Common errors in clinical measurement. *Anaesth. Intensiv. Care Med.* **2014**, *15*, 533–536.
50. Merit Sensor. *The Merit Sensor Blood Pressure Sensor*; Merit Sensor: South Jordan, UT, USA, 2015.
51. Elcam Medical. Elcam Disposable Integrated Pressure Transducer Is Indicated for Pressure Sensing During Clinically Invasive Procedures. Available online: http://www.elcam.co.il/pdf/pdf_brochure/Sense-IT(IPT)_2013.pdf (accessed on 3 May 2015).
52. Mems cap. *SP854 Biomedical Pressure Transducer*; Memscap Solutions: Crolles, France, 2012.
53. Measurement Specialties Inc. *Pressure Sensor—1620*; Measurement Specialties Inc.: Hampton, VA, USA, 2014.
54. Laine, S. FDA Approves First Implantable Wireless Device with Remote Monitoring to Measure Pulmonary Artery Pressure in Certain Heart Failure Patients. *FDA* **2014**. Available online: http://www.fda.gov/NewsEvents/Newsroom/PressAnnouncements/ucm399024.htm (accessed on 1 May 2015).
55. Roriz, P.; Ramos, A.; Santos, J.L.; Simões, J.A. Fiber optic intensity-modulated sensors: A review in biomechanics. *Photonic Sens.* **2012**, *2*, 315–330.
56. Faria, J.B. A theoretical analysis of the bifurcated fiber bundle displacement sensor. *IEEE Trans. Instrum. Meas.* **1998**, *47*, 742–747.

57. Brandao Faria, J. Modeling the Y-branched optical fiber bundle displacement sensor using a quasi-Gaussian beam approach. *Microw. Opt. Technol. Lett.* **2000**, *25*, 138–141.
58. Lekholm, A.; Lindström, L. Optoelectronic transducer for intravascular measurements of pressure variations. *Med. Biol. Eng.* **1969**, *7*, 333–335.
59. Lindstrom, L.H. Miniaturized pressure transducer intended for intravascular use. *IEEE Trans. Biomed. Eng.* **1970**, *BME-17*, 207–219.
60. Matsumoto, H.; Saegusa, M.; Saito, K.; Mizoi, K. The development of a fibre optic catheter tip pressure transducer. *J. Med. Eng. Technol.* **1978**, *2*, 239–242.
61. Crenshaw, A.G.; Styf, J.R.; Mubarak, S.J.; Hargens, A.R. A new "transducer-tipped" fiber optic catheter for measuring intramuscular pressures. *J. Orthop. Res.* **1990**, *8*, 464–468.
62. Shi, W. Fiber Optic Intravascular Blood Pressure Transducer. U.S. Patent 4,991,590, 12 February 1991.
63. Dianov, E.M.; Belovolov, M.I.; Bubnov, M.M.; Semenov, S.L. Fiber-Optic Pressure Sensor, Variants and Method for Producing A Resilient Membrane. U.S. Patent 6,539,136, 25 March 2003.
64. Little, R.L. Fiber Optic Pressure Transducer. U.S. Patent 5,005,584, 9 April 1991.
65. Fine, I.; Sternberg, A.; Katz, Y.; Goldinov, L.; Rapoport, B. Sensor, Method and Device for Optical Blood Oximetry. U.S. Patent 6,031,603, 29 February 2000.
66. Purdy, P.D.; Nair, A.; Pham, P.P.; Ramzipoor, K.; Bashiri, M.; Eder, J.C. Introducer Sheath. U.S. Patent 7,011,647, 14 March 2006.
67. Gelabert-Gonzalez, M.; Ginesta-Galan, V.; Sernamito-Garcia, R.; Allut, A.; Bandin-Dieguez, J.; Rumbo, R. The Camino Intracranial Pressure Device in Clinical Practice. Assessment in a 1000 Cases. *Acta Neurochir.* **2006**, *148*, 435–441.
68. Münch, E.; Weigel, R.; Schmiedek, P.; Schürer, L. The Camino intracranial pressure device in clinical practice: Reliability, handling characteristics and complications. *Acta Neurochir.* **1998**, *140*, 1113–1120.
69. Martínez-Mañas, R.M.; Santamarta, D.; de Campos, J.M.; Ferrer, E. Camino® intracranial pressure monitor: Prospective study of accuracy and complications. *J. Neurol. Neurosurg. Psychiatry* **2000**, *69*, 82–86.
70. Taffoni, F.; Formica, D.; Saccomandi, P.; Pino, G.D.; Schena, E. Optical fiber-based MR-compatible sensors for medical applications: An overview. *Sensors* **2013**, *13*, 14105–14120.
71. Hazarika, D.; Pegu, D. Micro-Controller based air pressure monitoring instrumentation system using optical fibers as sensor. *Opt. Fiber Technol.* **2013**, *19*, 83–87.
72. Johnson, D. Novel Optical Fibers-Draw-tower process creates high-quality FBG arrays. *Laser Focus World* **2012**, *48*, 53.
73. Lindner, E.; Mörbitz, J.; Chojetzki, C.; Becker, M.; Braückner, S.; Schuster, K.; Rothhardt, M.; Willsch, R.; Bartelt, H. Tailored draw tower fiber Bragg gratings for various sensing applications. *Proc. SPIE* **2012**, *8351*, doi:10.1117/12.913625.
74. Rao, Y.J. Recent progress in fiber-optic extrinsic Fabry–Perot interferometric sensors. *Opt. Fiber Technol.* **2006**, *12*, 227–237.

75. Udd, E.; Spillman, W.B., Jr. *Fiber Optic Sensors: An Introduction for Engineers and Scientists*; John Wiley & Sons: Hoboken, NJ, USA, 2011.
76. Lindner, E.; Canning, J.; Chojetzki, C.; Brückner, S.; Becker, M.; Rothhardt, M.; Bartelt, H. Post-hydrogen-loaded draw tower fiber Bragg gratings and their thermal regeneration. *Appl. Opt.* **2011**, *50*, 2519–2522.
77. Othonos, A.; Kalli, K. *Fiber Bragg Gratings: Fundamentals and Applications in Telecommunications and Sensing*; Artech House: Norwood, WI, USA, 1999.
78. Hill, K.O.; Meltz, G. Fiber Bragg Grating Technology Fundamentals and Overview. *J. Lightw. Technol.* **1997**, *15*, 1263–1276.
79. Lee, B. Review of the present status of optical fiber sensors. *Opt. Fiber Technol.* **2003**, *9*, 57–79.
80. Rao, Y.J. In-fibre Bragg grating sensors. *Meas. Sci. Technol.* **1997**, *8*, doi:10.1088/0957-0233/8/4/002.
81. LUNA. Optical Backscatter Reflectometer Model OBR 4600. Available online: http://lunainc.com/wp-content/uploads/ 2014/05/OBR4600_Data-Sheet_Rev-05.pdf (accessed on 11 May 2015).
82. Froggatt, M.E.; Gifford, D.K.; Kreger, S.; Wolfe, M.; Soller, B.J. Characterization of polarization-maintaining fiber using high-sensitivity optical-frequency-domain reflectometry. *J. Lightw. Technol.* **2006**, *24*, 4149–4154.
83. Bremer, K.; Leen, G.; Lewis, E.; Moss, B.; Lochmann, S.; Mueller, I. Pressure Sensor With an Interferometric Sensor and an in-Fiber Bragg Grating Reference Sensor. U.S. Patent 8,764,678, 1 July 2014.
84. Bae, H.; Yu, M. Miniature Fabry-Perot pressure sensor created by using UV-molding process with an optical fiber based mold. *Opt. Express* **2012**, *20*, 14573–14583.
85. Poeggel, S.; Leen, G.; Bremer, K.; Lewis, E. Miniature Optical fiber combined pressure-and temperature sensor for medical applications. In Proceedings of the 2012 IEEE Sensors, Taipei, Taiwan, 28–31 October 2012; pp. 1–4.
86. Tosi, D.; Macchi, E.G.; Braschi, G.; Cigada, A.; Gallati, M.; Rossi, S.; Poeggel, S.; Leen, G.; Lewis, E. Fiber-optic combined FPI/FBG sensors for monitoring of radio-frequency thermal ablation of liver tumors: *Ex vivo* experiments. *Appl. Opt.* **2014**, *53*, 2136–2144.
87. Poeggel, S.; Tosi, D.; Fusco, F.; Ippolito, J.; Lupoli, L.; Mirone, V.; Sannino, S.; Leen, G.; Lewis, E. Fiber-Optic EFPI Pressure Sensors for *In Vivo* Urodynamic Analysis. *IEEE Sens. J.* **2014**, *14*, 2335–2340.
88. Opsens. LifeSens. OpSens, IMP0030 LIFESENS Rev 2.0. Available online: http://www.opsens.com/pdf/products/LifeSens Rev 2_0.pdf (accessed on 5 May 2015).
89. Taffoni, F.; Formica, D.; Saccomandi, P.; Pino, G.D.; Schena, E. Optical fiber-based MR-compatible sensors for medical applications: An overview. *Sensors* **2013**, *13*, 14105–14120.
90. Rao, Y.J.; Jackson, D. Recent progress in fibre optic low-coherence interferometry. *Meas. Sci. Technol.* **1996**, *7*, 981–999.
91. Lee, B.H.; Kim, Y.H.; Park, K.S.; Eom, J.B.; Kim, M.J.; Rho, B.S.; Choi, H.Y. Interferometric fiber optic sensors. *Sensors* **2012**, *12*, 2467–2486.

92. Fabry, C.; Perot, A. Mesure de petites épaisseurs en valeur absolue. *Comptes Rendus* **1896**, *123*, 855–858.
93. Mishra, V.; Singh, N.; Tiwari, U.; Kapur, P. Fiber grating sensors in medicine: Current and emerging applications. *Sens. Actuators A Phys.* **2011**, *167*, 279–290.
94. Roriz, P.; Frazao, O.; Lobo-Ribeiro, A.B.; Santos, J.L.; Simoes, J.A. Review of fiber-optic pressure sensors for biomedical and biomechanical applications. *J. Biomed. Opt.* **2013**, *18*, doi:10.1117/1.JBO.18.5.050903.
95. Islam, M.R.; Ali, M.M.; Lai, M.H.; Lim, K.S.; Ahmad, H. Chronology of Fabry-Perot Interferometer Fiber-Optic Sensors and Their Applications: A Review. *Sensors* **2014**, *14*, 7451–7488.
96. Qi, B.; Pickrell, G.R.; Xu, J.; Zhang, P.; Duan, Y.; Peng, W.; Huang, Z.; Huo, W.; Xiao, H.; May, R.G.; *et al.* Novel data processing techniques for dispersive white light interferometer. *Opt. Eng.* **2003**, *42*, 3165–3171.
97. Chen, L.; Chan, C.; Yuan, W.; Goh, S.; Sun, J. High performance chitosan diaphragm-based fiber-optic acoustic sensor. *Sens. Actuators A Phys.* **2010**, *163*, 42–47.
98. Xu, F.; Ren, D.; Shi, X.; Li, C.; Lu, W.; Lu, L.; Lu, L.; Yu, B. High-sensitivity Fabry–Perot interferometric pressure sensor based on a nanothick silver diaphragm. *Opt. Lett.* **2012**, *37*, 133–135.
99. Li, C.; Xiao, J.; Guo, T.; Fan, S.; Jin, W. Interference characteristics in a Fabry–Perot cavity with graphene membrane for optical fiber pressure sensors. *Microsyst. Technol.* **2014**, doi:10.1007/s00542-014-2333-2.
100. Bae, H.; Yun, D.; Liu, H.; Olson, D.A.; Yu, M. Hybrid miniature Fabry–Perot sensor with dual optical cavities for simultaneous pressure and temperature measurements. *J. Lightw. Technol.* **2014**, *32*, 1585–1593.
101. FISO Technologies Inc. Evolution Product Datasheet – Medical Pressure Solution. Available online: http://www.fiso.com/admin/useruploads/files/fop-miv.pdf (accessed on 1 May 2015).
102. RJC Enterprises, LLC. Pressure Sensor Assemblies. Available online: http://www.rjcenterprises.net/products.html (accessed on 1 May 2015).
103. Kanellos, G.T.; Papaioannou, G.; Tsiokos, D.; Mitrogiannis, C.; Nianios, G.; Pleros, N. Two dimensional polymer-embedded quasi-distributed FBG pressure sensor for biomedical applications. *Opt. Express* **2010**, *18*, 179–186.
104. Ahmad, H.; Chong, W.Y.; Thambiratnam, K.; Zulklifi, M.Z.; Poopalan, P.; Thant, M.M.M.; Harun, S.W. High sensitivity fiber Bragg grating pressure sensor using thin metal diaphragm. *IEEE Sens. J.* **2009**, *9*, 1654–1659.
105. Zhang, W.; Li, F.; Liu, Y.; Liu, L. Ultrathin FBG pressure sensor with enhanced responsivity. *IEEE Photonics Technol. Lett.* **2007**, *19*, 1553–1555.
106. He, X.; Handa, J.; Gehlbach, P.; Taylor, R.; Iordachita, I. A submillimetric 3-DOF force sensing instrument with integrated fiber bragg grating for retinal microsurgery. *IEEE Trans. Biomed. Eng.* **2014**, *61*, 522–534.

107. Park, Y.L.; Ryu, S.C.; Black, R.J.; Moslehi, B.; Cutkosky, M.R. Fingertip force control with embedded fiber Bragg grating sensors. In Proceedings of the IEEE International Conference on Robotics and Automation, Pasadena, CA, USA, 19 May 2008; pp. 3431–3436.
108. Thompson, M.; Vandenberg, E.T. *In vivo* probes: Problems and perspectives. *Clin. Biochem.* **1986**, *19*, 255–261.
109. Rehman, S.; Claesson, A. Specialty optical fibers make surgery less invasive. *Photonics Spectra* **2012**, *38*, 10.
110. Roriz, P.; Carvalho, L.; Frazão, O.; Santos, J.L.; Simões, J.A. From conventional sensors to fibre optic sensors for strain and force measurements in biomechanics applications: A review. *J. Biomech.* **2014**, *47*, 1251–1261.
111. Mishra, V.; Singh, N. *Optical Fiber Gratings in Perspective of Their Applications in Biomedicine*; INTECH Open Access Publisher: Rijeka, Croatia, 2012.
112. Korolyov, V.; Potapov, V. Biomedical Fiber-Optic Temperature and Pressure Sensors. *Biomed. Eng.* **2012**, *46*, 1–4.
113. Cottler, P.S.; Karpen, W.R.; Morrow, D.A.; Kaufman, K.R. Performance characteristics of a new generation pressure microsensor for physiologic applications. *Ann. Biomed. Eng.* **2009**, *37*, 1638–1645.
114. Bosch, M.E.; Sánchez, A.J.R.; Rojas, F.S.; Ojeda, C.B. Recent development in optical fiber biosensors. *Sensors* **2007**, *7*, 797–859.
115. Dziuda, Ĺ. Fiber-optic sensors for monitoring patient physiological parameters: A review of applicable technologies and relevance to use during magnetic resonance imaging procedures. *J. Biomed. Opt.* **2015**, *20*, doi:10.1117/1.JBO.20.1.010901.
116. Peterson, J.; Vurek, G. Fiber-optic sensors for biomedical applications. *Science* **1984**, *224*, 123–127.
117. Hench, L.L.; Wilson, J. Biocompatibility of silicates for medical use. In *Silicon Biochemistry*; John Wiley: New York, NY, USA, 1986; pp. 231–246.
118. Voskerician, G.; Shive, M.S.; Shawgo, R.S.; von Recum, H.; Anderson, J.M.; Cima, M.J.; Langer, R. Biocompatibility and biofouling of MEMS drug delivery devices. *Biomaterials* **2003**, *24*, 1959–1967.
119. Kotzar, G.; Freas, M.; Abel, P.; Fleischman, A.; Roy, S.; Zorman, C.; Moran, J.M.; Melzak, J. Evaluation of MEMS materials of construction for implantable medical devices. *Biomaterials* **2002**, *23*, 2737–2750.
120. Li, Y.; Shawgo, R.S.; Tyler, B.; Henderson, P.T.; Vogel, J.S.; Rosenberg, A.; Storm, P.B.; Langer, R.; Brem, H.; Cima, M.J. *In vivo* release from a drug delivery MEMS device. *J. Controlled Release* **2004**, *100*, 211–219.
121. Lavan, D.A.; McGuire, T.; Langer, R. Small-scale systems for *in vivo* drug delivery. *Nat. Biotechnol.* **2003**, *21*, 1184–1191.
122. Yang, C.; Zhao, C.; Wold, L.; Kaufman, K.R. Biocompatibility of a physiological pressure sensor. *Biosens. Bioelectron.* **2003**, *19*, 51–58.

123. OFS. Fiber Opticl Solutions for Medical Devices. Available online: http://www.ofsoptics.com/pdf/fiber_optic_solutions_for_medical_devices.pdf (accessed on 6 July 2015).
124. Stolov, A.A.; Slyman, B.E.; Burgess, D.T.; Hokansson, A.S.; Li, J.; Allen, R.S. Effects of sterilization methods on key properties of specialty optical fibers used in medical devices. *Proc. SPIE* **2013**, *8576*, doi:10.1117/12.1000005.
125. Everhart, J.E.; Ruhl, C.E. Burden of digestive diseases in the United States part I: Overall and upper gastrointestinal diseases. *Gastroenterology* **2009**, *136*, 376–386.
126. Peery, A.F.; Dellon, E.S.; Lund, J.; Crockett, S.D.; McGowan, C.E.; Bulsiewicz, W.J.; Gangarosa, L.M.; Thiny, M.T.; Stizenberg, K.; Morgan, D.R.; *et al*. Burden of Gastrointestinal Disease in the United States: 2012 Update. *Gastroenterology* **2012**, *143*, 1179–1187.
127. Takeuchi, S.; Tohara, H.; Kudo, H.; Otsuka, K.; Saito, H.; Uematsu, H.; Mitsubayashi, K. An optic pharyngeal manometric sensor for deglutition analysis. *Biomed. Microdevices* **2007**, *9*, 893–899.
128. Kong, D.R.; He, B.B.; Wu, A.J.; Wang, J.G.; Yu, F.F.; Xu, J.M. Fiberoptic sensor for noninvasive measurement of variceal pressure. *Endoscopy* **2013**, *45*, E55–E56.
129. Arkwright, J.W.; Underhill, I.D.; Maunder, S.A.; Blenman, N.; Szczesniak, M.M.; Wiklendt, L.; Cook, I.J.; Lubowski, D.Z.; Dinning, P.G. Design of a high-sensor count fibre optic manometry catheter for *in vivo* colonic diagnostics. *Opt. Express* **2009**, *17*, 22423–22431.
130. Arkwright, J.W.; Blenman, N.G.; Underhill, I.D.; Maunder, S.A.; Szczesniak, M.M.; Dinning, P.G.; Cook, I.J. *In-vivo* demonstration of a high resolution optical fiber manometry catheter for diagnosis of gastrointestinal motility disorders. *Opt. Express* **2009**, *17*, 4500–4508.
131. Wang, D.H.C.; Abbott, A.; Maunder, S.A.; Blenman, N.G.; Arkwright, J.W. A miniature fiber Bragg grating pressure sensor for *in vivo* sensing applications. *Proc. SPIE* **2012**, *8421*, doi:10.1117/12.967696.
132. Becker, M.; Rothhardt, M.; Schröder, K.; Voigt, S.; Mehner, J.; Teubner, A.; Lüpke, T.; Thieroff, C.; Krüger, M.; Chojetzki, C.; *et al.* Characterization of fiber Bragg grating-based sensor array for high resolution manometry. *Proc. SPIE* **2012**, *8439*, doi:10.1117/12.921830.
133. Dinning, P.; Wiklendt, L.; Maslen, L.; Gibbins, I.; Patton, V.; Arkwright, J.; Lubowski, D.; O'Grady, G.; Bampton, P.; Brookes, S.; *et al*. Quantification of *in vivo* colonic motor patterns in healthy humans before and after a meal revealed by high-resolution fiber-optic manometry. *Neurogastroenterol. Motil.* **2014**, *26*, 1443–1457.
134. Roger, V.L.; Go, A.S.; Lloyd-Jones, D.M.; Benjamin, E.J.; Berry, J.D.; Borden, W.B.; Bravata, D.M.; Dai, S.; Ford, E.S.; Fox, C.S.; *et al*. Heart disease and stroke statistics—2012 update a report from the American heart association. *Circulation* **2012**, *125*, e2–e220.
135. Go, A.S.; Mozaffarian, D.; Roger, V.L.; Benjamin, E.J.; Berry, J.D.; Blaha, M.J.; Dai, S.; Ford, E.S.; Fox, C.S.; Franco, S.; *et al*. Heart disease and stroke statistics–2014 update: A report from the American Heart Association. *Circulation* **2014**, *129*, doi: 10.1161/01.cir.0000441139.02102.80.
136. Reesink, K.D.; van der Nagel, T.; Bovelander, J.; Jansen, J.R.; van der Veen, F.H.; Schreuder, J.J. Feasibility study of a fiber-optic system for invasive blood pressure measurements. *Catheter. Cardiovasc. Interv.* **2002**, *57*, 272–276.

137. Woldbaek, P.R.; Strømme, T.A.; Sande, J.B.; Christensen, G.; Tønnessen, T.; Ilebekk, A. Evaluation of a new fiber-optic pressure recording system for cardiovascular measurements in mice. *Am. J. Physiol. Heart Circulatory Physiol.* **2003**, *285*, H2233–H2239.
138. Schreuder, J.J.; Castiglioni, A.; Donelli, A.; Maisano, F.; Jansen, J.R.; Hanania, R.; Hanlon, P.; Bovelander, J.; Alfieri, O. Automatic Intraaortic Balloon Pump Timing Using an Intrabeat Dicrotic Notch Prediction Algorithm. *Ann. Thoracic Surg.* **2005**, *79*, 1017–1022.
139. Pinet, E.; Pham, A.; Rioux, S. Miniature fiber optic pressure sensor for medical applications: An opportunity for intra-aortic balloon pumping (IABP) therapy. *Proc. SPIE* **2005**, *5855*, 234–237.
140. Yarham, G.; Clements, A.; Morris, C.; Cumberland, T.; Bryan, M.; Oliver, M.; Burrows, H.; Mulholland, J. Fiber-optic intra-aortic balloon therapy and its role within cardiac surgery. *Perfusion* **2013**, *28*, 97–102.
141. Schock, R.; Williams, J.; Walters, D. Intra-aortic balloon catheter having a dual sensor pressure sensing system. US patent 7,229,403, 12 June 2007.
142. Mulholland, J.; Yarham, G.; Clements, A.; Morris, C.; Loja, D. Mechanical left ventricular support using a 50 cc 8 Fr fibre-optic intra-aortic balloon technology: A case report. *Perfusion* **2013**, *28*, 109–113.
143. Wu, N.; Tian, Y.; Zou, X.; Zhai, Y.; Barringhaus, K.; Wang, X. A miniature fiber optic blood pressure sensor and its application in *in vivo* blood pressure measurements of a swine model. *Sens. Actuators B Chem.* **2013**, *181*, 172–178.
144. Yuan, Q.Y.; Zhang, L.; Xiao, D.; Zhao, K.; Lin, C.; Si, L.Y. An Accurate, Flexible and Small Optical Fiber Sensor: A Novel Technological Breakthrough for Real-Time Analysis of Dynamic Blood Flow Data *In Vivo*. *PLoS ONE* **2014**, *9*, doi:10.1371/journal.pone.0114794.
145. Tian, Y.; Wu, N.; Zou, X.; Zhang, Y.; Barringhaus, K.; Wang, X. A Study on Packaging of Miniature Fiber Optic Sensors for *In-Vivo* Blood Pressure Measurements in a Swine Model. *IEEE Sens. J.* **2014**, *14*, 629–635.
146. Tucker-Schwartz, J.; Gillies, G.; Mahapatra, S. Improved Pressure Frequency Sensing Subxiphoid Pericardial Access System: Performance Characteristics During *in Vivo* Testing. *IEEE Trans. Biomed. Eng.* **2011**, *58*, 845–852.
147. Bakker, E.; Visser, K.; Van Der Wal, A.; Kuiper, M.; Koopmans, M.; Breedveld, R. Inflation and deflation timing of the AutoCAT 2 WAVE intra-aortic balloon pump using the autoPilot mode in a clinical setting. *Perfusion* **2012**, *27*, 393–398.
148. Hanlon-Pena, P.M.; Quaal, S.J. Resource Document: Evidence Supporting Current Practice in Timing Assessment. *Am. J. Crit. Care* **2011**, *20*, e99–e102.
149. Rodriguez, D.A.A.; Durand, E.; de Rochefort, L.; Boudjemline, Y.; Mousseaux, E. Simultaneous pressure-volume measurements using optical sensors and MRI for left ventricle function assessment during animal experiment. *Med. Eng. Phys.* **2015**, *37*, 100–108.
150. Rodriguez, D. Left Ventricular Pressure-Volume Analysis: An Example of Function Assessment on a Sheep. Ph.D. Thesis, Université Paris Sud, Paris, France, 2015.
151. Reilly, P.; Bullock, R. *Head Injury: Pathophysiology & Management*, 2nd ed.; CRC Press: Boca Raton, FL, USA, 2005.

152. Shapiro, S.; Bowman, R.; Callahan, J.; Wolfla, C. The fiberoptic intraparenchymal cerebral pressure monitor in 244 patients. *Surg. Neurol.* **1996**, *45*, 278–281.
153. Bekar, A.; Dogan, S.; Abas, F.; Caner, B.; Korfali, G.; Kocaeli, H.; Yilmazlar, S.; Korfali, E. Risk factors and complications of intracranial pressure monitoring with a fiberoptic device. *J. Clin. Neurosci.* **2009**, *16*, 236–240.
154. Chavko, M.; Koller, W.A.; Prusaczyk, W.K.; McCarron, R.M. Measurement of blast wave by a miniature fiber optic pressure transducer in the rat brain. *J. Neurosci. Methods* **2007**, *159*, 277–281.
155. Leonardi, A.D.C.; Bir, C.A.; Ritzel, D.V.; VandeVord, P.J. Intracranial pressure increases during exposure to a shock wave. *J. Neurotrauma* **2011**, *28*, 85–94.
156. Dal Cengio Leonardi, A.; Keane, N.; Hay, K.; Ryan, A.; Bir, C.; VandeVord, P. Methodology and Evaluation of Intracranial Pressure Response in Rats Exposed to Complex Shock Waves. *Ann. Biomed. Eng.* **2013**, *41*, 2488–2500.
157. Bir, C. *Measuring Blast-Related Intracranial Pressure within the Human Head*; Technical Report; DTIC Document: Detroit, MI, USA, 2011.
158. Nitti, V.W. Pressure flow urodynamic studies: The gold standard for diagnosing bladder outlet obstruction. *Rev. Urol.* **2005**, *7*, S14–S21.
159. Defreitas, G.A.; Zimmern, P.E.; Lemack, G.E.; Shariat, S.F. Refining diagnosis of anatomic female bladder outlet obstruction: Comparison of pressure-flow study parameters in clinically obstructed women with those of normal controls. *Urology* **2004**, *64*, 675–679.
160. Belville, W.D.; Swierzewski, S.J.; Wedemeyer, G.; McGuire, E.J. Fiberoptic microtransducer pressure technology: Uurodynamic implications. *Neurourol. Urodyn.* **1993**, *12*, 171–178.
161. Poeggel, S.; Duraibabu, D.; Tosi, D.; Leen, G.; Lewis, E.; McGrath, D.; Fusco, F.; Sannino, S.; Lupoli, L.; Ippolito, J.; *et al.* Differential *in vivo* urodynamic measurement in a single thin catheter based on two optical fiber pressure sensors. *J. Biomed. Opt.* **2015**, *20*, doi:10.1117/1.JBO.20.3.037005.
162. Olson, E.S.; Nakajima, H.H. A family of fiber-optic based pressure sensors for intracochlear measurements. *Proc. SPIE* **2015**, *9303*, doi:10.1117/12.2178056.
163. Tjin, S.; Tan, Y.; Yow, M.; Lam, Y.Z.; Hao, J. Recording compliance of dental splint use in obstructive sleep apnoea patients by force and temperature modelling. *Med. Biol. Eng. Comput.* **2001**, *39*, 182–184.
164. Weber, J.R.; Baribeau, F.; Grenier, P.; Émond, F.; Dubois, S.; Duchesne, F.; Girard, M.; Pope, T.; Gallant, P.; Mermut, O.; *et al*. Towards a bimodal proximity sensor for *in situ* neurovascular bundle detection during dental implant surgery. *Biomed. Opt. Express* **2014**, *5*, 16–30.
165. Zhong, L.; Bradley, J.; Schubert, W.; Ahmed, E.; Adamis, A.P.; Shima, D.T.; Robinson, G.S.; Ng, Y.S. Erythropoietin promotes survival of retinal ganglion cells in DBA/2J glaucoma mice. *Investig. Ophthalmol. Vis. Sci.* **2007**, *48*, 1212–1218.
166. Leung, L.K.; Ko, M.W.; Lam, D.C. Individual-specific tonometry on porcine eyes. *Med. Eng. Phys.* **2014**, *36*, 96–101.

167. Liu, X.; Iordachita, I.I.; He, X.; Taylor, R.H.; Kang, J.U. Miniature fiber-optic force sensor based on low-coherence Fabry-Perotrot interferometry for vitreoretinal microsurgery. *Biomed. Opt. Express* **2012**, *3*, 1062–1076.
168. Gonenc, B.; Gehlbach, P.; Handa, J.; Taylor, R.H.; Iordachita, I. Force-Sensing Microneedle for Assisted Retinal Vein Cannulation. In Proceedings of IEEE Sensors/IEEE International Conference on Sensors, Valencia, Spain, 2–5 November 2014; pp. 698–701.
169. Ferreira, L.A.; Araujo, F.M.; Mascarenhas, T.; Natal Jorge, R.M.; Fernandes, A.A. Dynamic assessment of women pelvic floor function by using a fiber Bragg grating sensor system. *Proc. SPIE* **2006**, *6083*, doi:10.1117/12.646824.
170. Inokuchi, W.; Olsen, B.S.; Sojbjerg, J.O.; Sneppen, O. The relation between the position of the glenohumeral joint and the intraarticular pressure: An experimental study. *J. Shoulder Elbow Surg.* **1997**, *6*, 144–149.
171. Cottler, P.S.; Blevins, D.; Averett, J.; Wavering, T.A.; Morrow, D.A.; Shin, A.Y.; Kaufman, K.R. Miniature optical fiber pressure microsensors for *in vivo* measurement of intramuscular pressure. *Proc. SPIE* **2007**, *6433*, doi:10.1117/12.700989.
172. Nilsson, A.; Zhang, Q.; Styf, J. The amplitude of pulse-synchronous oscillations varies with the level of intramuscular pressure in simulated compartment syndrome. *J. Exp. Orthop.* **2015**, *2*, doi:10.1186/s40634-015-0020-6.
173. Li, J.; Hammer, S.; Shu, W.; Maier, R.; Hand, D.; Reuben, R.; MacPherson, W. An optical fibre dynamic instrumented palpation sensor for the characterisation of biological tissue. *Sens. Actuators A Phys.* **2015**, *225*, 53–60.
174. Roriz, P.; Ferreira, J.M.C.; Potes, J.C.; Oliveira, M.T.; Frazao, O.; Santos, J.L.; Simoes, J.A.D.O. *In vivo* measurement of the pressure signal in the intervertebral disc of an anaesthetized sheep. *J. Biomed. Opt.* **2014**, *19*, doi:10.1117/1.JBO.19.3.037006.
175. De Blast, R.; Conti, G.; Antonelli, M.; Bufi, M.; Gasparetto, A. A fibre optics system for the evaluation of airway pressure in mechanically ventilated patients. *Intensiv. Care Med.* **1992**, *18*, 405–409.
176. Sondergaard, S.; Karason, S.; Hanson, A.; Nilsson, K.; Hojer, S.; Lundin, S.; Stenqvist, O. Direct measurement of intratracheal pressure in pediatric respiratory monitoring. *Pediatric Res.* **2002**, *51*, 339–345.
177. Hogan, J.; Mintchev, M. Method and Apparatus for Intra-oesophageal Cough Detection. In Proceedings of the 28th Annual International Conference of the IEEE Engineering in Medicine and Biology Society, New York, NY, USA, 30 August–3 September 2006; pp. 551–554.
178. Wood, B.J.; Ramkaransingh, J.R.; Fojo, T.; Walther, M.M.; Libutti, S.K. Percutaneous tumor ablation with radio-frequency. *Cancer* **2002**, *94*, 443–451.
179. Solbiati, L.; Livraghi, T.; Goldberg, S.N.; Ierace, T.; Meloni, F.; Dellanoce, M.; Cova, L.; Halpern, E.F.; Gazelle, G.S. Percutaneous radio-frequency ablation of hepatic metastases from colorectal cancer: Long-term results in 117 patients 1. *Radiology* **2001**, *221*, 159–166.
180. Sapareto, S.A.; Dewey, W.C. Thermal dose determination in cancer therapy. *Int. J. Radiat. Oncol. Biol. Phys.* **1984**, *10*, 787–800.

181. Kotoh, K.; Nakamuta, M.; Morizono, S.; Kohjima, M.; Arimura, E.; Fukushima, M.; Enjoji, M.; Sakai, H.; Nawata, H. A multi-step, incremental expansion method for radio frequency ablation: Optimization of the procedure to prevent increases in intra-tumor pressure and to reduce the ablation time. *Liver Int.* **2005**, *25*, 542–547.
182. Tosi, D.; Macchi, E.G.; Cigada, A. Fiber-Optic Temperature and Pressure Sensors Applied to Radiofrequency Thermal Ablation in Liver Phantom: Methodology and Experimental Measurements. *J. Sens.* **2015**, *2015*, pp. 1–22.
183. Poeggel, S.; Tosi, D.; Leen, G.; Lewis, E. Low drift and high resolution miniature optical fiber combined pressure- and temperature sensor for cardio-vascular and other medical applications. In Proceedings of the 2013 IEEE Sensors, Baltimore, MD, USA, 3–6 November 2013; pp. 1–4.
184. Kokkinos, D.; Dehipawala, S.; Holden, T.; Cheung, E.; Musa, M.; Tremberger, G., Jr.; Schneider, P.; Lieberman, D.; Cheung, T. Fiber optic based heart-rate and pulse pressure shape monitor. *Proc. SPIE* **2012**, *8218*, doi:10.1117/12.909582.
185. Van Brakel, A.; Swart, P.L.; Chtcherbakov, A.A.; Shlyagin, M.G. Blood pressure manometer using a twin Bragg grating Fabry-Perot interferometer. *Proc. SPIE* **2005**, *5634*, 595–602.
186. Mo, Z.; Xu, W.; Broderick, N. A Fabry-Perot optical fiber force sensor based on intensity modulation for needle tip force sensing. In Proceedings of the 2015 6th International Conference on Automation, Robotics and Applications (ICARA), Queenstown, New Zealand, 17–19 February 2015; pp. 376–380.
187. Dennison, C.R.; Wild, P.M.; Byrnes, P.W.; Saari, A.; Itshayek, E.; Wilson, D.C.; Zhu, Q.A.; Dvorak, M.F.; Cripton, P.A.; Wilson, D.R. *Ex vivo* measurement of lumbar intervertebral disc pressure using fibre-Bragg gratings. *J. Biomech.* **2008**, *41*, 221–225.
188. Chen, Z.; Lau, D.; Teo, J.T.; Ng, S.H.; Yang, X.; Kei, P.L. Simultaneous measurement of breathing rate and heart rate using a microbend multimode fiber optic sensor. *J. Biomed. Opt.* **2014**, *19*, doi:10.1117/1.JBO.19.5.057001.
189. Hao, J.; Jayachandran, M.; Kng, P.; Foo, S.; Aung, P.; Cai, Z. FBG-based smart bed system for healthcare applications. *Front. Optoelectron. China* **2010**, *3*, 78–83.
190. Nishyama, M.; Miyamoto, M.; Watanabe, K. Respiration and body movement analysis during sleep in bed using hetero-core fiber optic pressure sensors without constraint to human activity. *J. Biomed. Opt.* **2011**, *16*, doi:10.1117/1.3528008.
191. Dziuda, L.; Skibniewski, F.W.; Krej, M.; Lewandowski, J. Monitoring respiration and cardiac activity using fiber Bragg grating-based sensor. *IEEE Trans. Biomed. Eng.* **2012**, *59*, 1934–1942.
192. Swart, P.L.; Lacquet, B.M.; Chtcherbakov, A.A. A fiber optic oesophageal pressure sensor. *Proc. SPIE* **2004**, *5502*, 120–123.
193. Dziuda, L.; Skibniewski, F.W.; Krej, M.; Baran, P.M. Fiber Bragg grating-based sensor for monitoring respiration and heart activity during magnetic resonance imaging examinations. *J. Biomed. Opt.* **2013**, *18*, doi:10.1117/1.JBO.18.5.057006.
194. Samba Sensors. *Exactly, How Accurate Pressure Data Do You Need?*; Harvard Apparatus Canada: St. Laurent, Quebec, Canada, 2007.
195. Camino. *OLM IntracraData pressure monitoring kit Model 110-4B*; Integra NeuroSciences Camino: San Diego, CA, USA, 1998.

196. Maquet. *CS300 IABP Product Features*; Maquet Getinge Group: Mahwah, NJ, USA.
197. Harada, M.; Qin, Y.; Takano, H.; Minamino, T.; Zou, Y.; Toko, H.; Ohtsuka, M.; Matsuura, K.; Sano, M.; Nishi, J.I.; *et al*. G-CSF prevents cardiac remodeling after myocardial infarction by activating the Jak-Stat pathway in cardiomyocytes. *Nat. Med.* **2005**, *11*, 305–311.
198. Krave, U.; Höjer, S.; Hansson, H.A. Transient, powerful pressures are generated in the brain by a rotational acceleration impulse to the head. *Eur. J. Neurosci.* **2005**, *21*, 2876–2882.
199. Murtha, L.; McLeod, D.; Spratt, N. Epidural Intracranial Pressure Measurement in Rats Using a Fiber-optic Pressure Transducer. *J. Vis. Exp.* **2012**, doi:10.3791/3689.
200. Hoejer, S.; Krantz, M.; Ekstroem, L.; Kaigle, A.; Holm, S. Microstructure-based fiber optic pressure sensor for measurements in lumbar intervertebral discs. *Proc. SPIE* **1999**, *3570*, doi:10.1117/12.336921.
201. Nazarian, S.; Kolandaivelu, A.; Zviman, M.M.; Meininger, G.R.; Kato, R.; Susil, R.C.; Roguin, A.; Dickfeld, T.L.; Ashikaga, H.; Calkins, H.; *et al*. Feasibility of real-time magnetic resonance imaging for catheter guidance in electrophysiology studies. *Circulation* **2008**, *118*, 223–229.
202. Casanova, F.; Carney, P.R.; Sarntinoranont, M. Effect of Needle Insertion Speed on Tissue Injury, Stress, and Backflow Distribution for Convection-Enhanced Delivery in the Rat Brain. *PLoS ONE* **2014**, *9*, doi:10.1371/journal.pone.0094919.
203. Lescot, T.; Reina, V.; Le Manach, Y.; Boroli, F.; Chauvet, D.; Boch, A.L.; Puybasset, L. *In vivo* accuracy of two intraparenchymal intracranial pressure monitors. In *Applied Physiology in Intensive Care Medicine 1*; Springer: Berlin Heidelberg, Germany, 2012; pp. 249–253.
204. Kim, M.; Edlow, B.; Durduran, T.; Frangos, S.; Mesquita, R.; Levine, J.; Greenberg, J.; Yodh, A.; Detre, J. Continuous Optical Monitoring of Cerebral Hemodynamics During Head-of-Bed Manipulation in Brain-Injured Adults. *Neurocrit. Care* **2014**, *20*, 443–453.
205. Crenshaw, A.; Styf, J.; Hargens, A. Intramuscular pressures during exercise: An evaluation of a fiber optic transducer-tipped catheter system. *Eur. J. Appl. Physiol. Occup. Physiol.* **1992**, *65*, 178–182.
206. Pedowitz, R.A.; Gershuni, D.H.; Crenshaw, A.G.; Petras, S.L.; Danzig, L.A.; Hargens, A.R. Intraarticular pressure during continuous passive motion of the human knee. *J. Orthop. Res.* **1989**, *7*, 530–537.
207. Nair, P.K.; Scolieri, S.; Lee, A.B. What's Trending. *J. Invasiv. Cardiol.* **2011**, *23*, 162–166.